8-26-2019

Liquid Crystalline Brush-like Imidazolium Co-polymer Membranes For Energy Conversion

Edirimuni Iyomali Abeysekera
iyomali.abeysekera@uconn.edu

Liquid Crystalline Brush-like Imidazolium Copolymer Membranes for Energy Conversion

Edirimuni Iyomali Abeysekera

B.Sc., University of Peradeniya, Sri Lanka, 2017

A Thesis

Submitted in Partial Fulfillment of the

Requirements for the Degree of

Master of Science

At the

University of Connecticut

2019

APPROVAL PAGE

Masters of Science Thesis

Liquid Crystalline Brush-like Imidazolium Copolymer Membranes for Energy Conversion

Presented by

Edirimuni Iyomali Abeysekera, B.Sc.

Major Advisor _____

Prof. Rajeswari M. Kasi

Associate Advisor _____

Prof. Douglas Adamson

Associate Advisor _____

Prof. Yao Lin

University of Connecticut

2019

Acknowledgments

I express my sincere gratitude to my advisor Prof. Rajeswari M. Kasi for giving me a wonderful opportunity to work in her laboratory and for the tremendous academic support, guidance and suggestions given throughout the past two years. I would like to thank her for giving me the freedom to work enthusiastically with our teaching duties and course work and always encouraging and motivating me to think independently and to make good collaborations with others.

I am also thankful to my committee Prof. Douglas Adamson and Prof. Yao Lin for being extremely supportive and for being the part of my committee in spite of their busy schedules.

My special thank goes to my mentors Dennis and Reuben who gave me tremendous support to be successful in my research work from the very first day. Also, my sincere gratitude goes to my other lab mates Ian, Sameeksha and Ashish for their valuable suggestions and discussions throughout these two years. I am very thankful to all the chemistry department staff and Institute of material's science staff especially Emilie, Charlene, Nancy, Osker, Josh and Sandra from registrar's office for assisting me with all the administrative work. Special thanks go to my family and friends for being extremely supportive and encouraging me through the rough days. Finally, I would like to thank the University of Connecticut, the Chemistry department and all my funding agencies for the support.

Table of Contents

List of Figures

List of Schemes

List of Tables

Abstract

Anion exchange membrane (AEM) research is primarily focused to develop suitable AEMs with high ion conductivity for high pH and high-temperature environments used in water electrolysis and fuel cells. To address these issue research has been done on improving the ion exchange head group to obtain high ion conductivity and designing a rational polymer architecture to improve chemical and mechanical stability.

Most widely used ionic head groups are based on quaternary ammonium ions due to its high ion conductivity. However quaternary ammonium ion containing membranes degrades with time resulting in low ion exchange capacity (IEC) and low alkaline stability due to its susceptibility to hydroxide ions. Therefore, branching out from quaternary ammonium ion-based membranes research has been widely done on other N containing cations such as imidazolium, pyridinium and guanidium. Out of these imidazolium has shown the most assurance due to its high ion conductivity and adaptable structure for modifications.

In parallel with enhancing the chemistry of the ion exchange moiety research has been done improving the polymer architecture to gain more chemical and mechanical stability. Most widely used polymer backbones are polysulfones and fluorinated polymers, Nafion being the most popular. Nevertheless, literature has highlighted a few major drawbacks of polymer membranes synthesized with these. Polysulfones are susceptible to ether and quaternary carbon hydrolysis and polyfluorines are subjected to dehydrofluorination with time. As a result, research has been done on many other polymer backbones and polynorbornene has attracted much attention due to it's high thermal and chemical stability, excellent film-forming properties and simple controllable polymerization techniques.

One important strategy to obtain ion conductivity includes having densely functionalized ion-conducting groups on a hydrophobic polymer matrix creating ion channels. Also rather than attaching the ion exchanging head group directly to the polymer backbone having it on regularly spaced flexible side chains improves ion conductivity. Apart from that this architecture is promised to show more alkaline stability due to the polymer backbone being protected by the hydrophobic polymer matrix.

Considering all these facts it is clear that both ion exchange head group and polymer architecture are equally important in designing an AEMs addressing the current issues in the field. In this work we present a series of a novel brush like liquid crystalline imidazolium functionalized norbornene ionic liquid copolymers with ion channels and improved alkaline stability.

Chapter one – Introduction

1.1 Man's quest for Energy

Energy is one of the three main components needed to ensure human survival and has become the key to rapid industrial growth and technological development. Since primitive humans began to utilize firewood it has been a crucial factor for human existence. With advances in technology, humankind has been looking for other efficient energy sources and the discovery of ordinary black coal, which is an energy-rich hydrocarbon caused an epochal change in human history.

Invasion of coal associated with steam engines accelerated the progress in human civilization in many ways. In 1780s coal contributed to the greatest share of the world's energy consumption exceeding wood for the first time.[1] The pace of development after the industrial revolution was outstanding and the demand for energy accelerated due to the enhanced quality of life and industrial development. A century later oils and other gases came into the play to gratify the thirst of industry. This further increased the industrialization of both developed and developing countries and increasing the world population drastically. World's energy consumption mainly rely on the level of socio-economic growth and the ability to retrieve the sources. As a result, coal and other high carbon energy sources such as petroleum expanded manifolds and it is estimated that if the fossil fuel usage remains increasing fossil fuel reserves will be depleted by 2050.[2]

Apart from this environmental, health and ecological problems originated due to the utilization of fossil fuels have become increasingly notable in the recent past. The climate change due to greenhouse gas emission, increase in the level of ultraviolet light due to the breakdown of the ozone layer, acid rains, decrease in biodiversity, soil erosion and water contamination are some such issues.[3]

As a result of the large energy demand plus the interest towards the green energy recently most research work has focused their interest on alternative renewable energy sources such as hydro, nuclear, geothermal, solar, wind and biogas. However, these eco-friendly energy sources contribute to only 15% of the global energy demand due to them not being exploited adequately because of cost, technological barriers, and political issues. This makes fossil fuel still the number one source of energy despite the harm it does to the environment. Considering all these facts the world's energy demand and development is invading a new era where clean and low carbon energy is unavoidable and has sparked fresh enthusiasm improving electrochemical devices to generate energy. Fuel cells, electrolyzers, and flow batteries are considered to be the most competitive and promising in the upcoming energy-conversion field.[4,5]

Among these fuel cells are on the edge of creating a revolutionary change in global energy production and storage due to its high efficiency and cost-effective supply of power as a green source of energy.[6]

1.2 Fuel cells

By definition fuel cell is an electrochemical device which directly converts chemical energy into electrical energy by combining fuel with an oxidant like oxygen from air by the help of electrodes and an ion conducting electrolyte. During this process, water is formed as a byproduct.[7] The principal feature of the fuel cell is it converts chemical energy to electricity and heat without combustion of the fuel and thus they are environmentally friendly. Also compared to conventional heat engines traditionally used for this purpose wastes a considerable amount of energy as mechanical energy resulting in low energy conversion efficiencies. The other advantage is unlike a battery it does not require any recharging and runs continuously as long as fuel is pumped.[8] Hydrogen, methanol, ethanol and ethylene glycol are the most widely used fuels.

Fuel cells may be categorized into many based on the type of the reactant (considering different types of fuels and oxidant), type of electrolyte, type of the exchanged ion through the electrolyte, operating conditions, etc. Generally, fuel cells are classified based on the type of the electrolyte used and following are the five main types of fuel cells in use as of now.[9]

(1). Alkaline fuel cells (AFC) - uses Potassium hydroxide (KOH) as the electrolyte

(2). Phosphoric acid fuel cells (PAFC) – uses Phosphoric acid as the electrolyte

(3). Polymer electrolyte membrane fuel cells (PEMFC) – consist of an ion exchange membrane as the electrolyte.

(4). Molten carbonate fuel cells (MCFC) – uses molted carbonate salt as the electrolyte

(5). Solid oxide fuel cells (SOFC) – Uses inorganic oxides as the electrolyte

Among these PEMFCs has evoked the enthusiasm of researches around the world due to its expansion into the synthesis of a vast range of materials and the ability to modify the architectures accordingly to obtain desired properties.

In general ion exchange membrane is the key segment of a fuel cell. Ion exchange membranes are semi-permeable membranes containing anionic head group attached to a polymer matrix. [10] The main function of the membrane is to transport ions with a minimum resistance possible but it also functions as a wall to separate the reactant gases. In PEMFCs either an anion exchange membrane or cation exchange membrane is used as the electrolyte. Cation exchange membranes(CEMs) contains negatively charged ionic head groups such as SO_3^-, CO_3^{2-}, and PO_3^{2-} attached to the polymer matrix selectively allowing the passage of cations only. On the other hand, anion exchange membranes contain positively charged head groups such as quaternary ammonium ions

fixed to the polymeric backbone allowing the passage of anions, rejecting cations. Until recent past proton exchange membrane (PEM) fuel cells have shown the greatest promise compared to AEMFCs and been the leading technology in the fuel cell industry.

1.2.1 Proton exchange membrane fuel cells

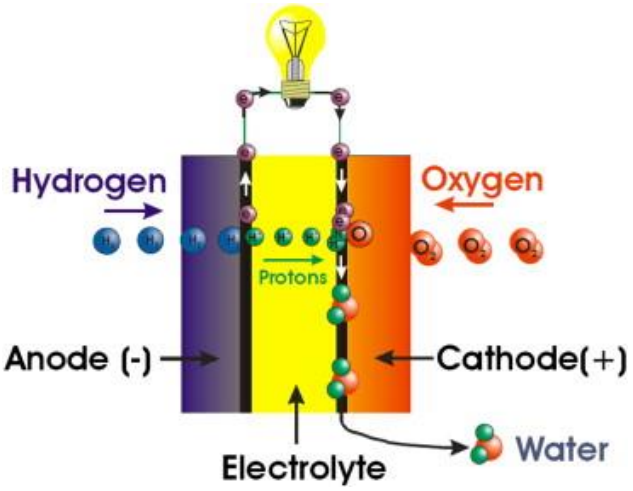

Figure 1. 1: Schematic illustration of a proton exchange membrane fuel cell. Adapted from reference (9)

Hydrogen gas is charged to the anode where it contacts a catalytic surface which facilitates the splitting it into hydrogen ions and electrons. These protons move through the cation exchange membrane to the cathode and electrons move through a circuit towards cathode due to an electric potential gradient to produce an electric current.

Anode reaction: $H_2 \longrightarrow 2H^+ + 2e^-$

Cathode reaction: $O_2 + 4H^+ + 4e^- \longrightarrow 2H_2O$

Overall reaction: $2H_2 + O_2 \longrightarrow 2H_2O$

The main reason for PEM fuel cells to be the most promising technology over the past century is the ability to create cation exchange membranes with high proton conductivities. For instance, Nafion 117 introduced by Dupont in 1970s has hit the market with a proton conductivity as high as 78 mS/cm at 100% relative humidity.[11]

Nafion is a sulfonated tetrafluoroethylene copolymer and is produced by copolymerization of different amounts of unsaturated perfluoroalkyl sulfonyl fluoride with tetrafluoroethylene. The poly(tetrafluoroethylene) backbone gives it's exceptionally high chemical resistance and the ability to operate at fairly high temperatures as high as 190˚C.[12] Its high stability is mainly due to the presence of C-F bond which has a high bond dissociation enthalpy (464 KJ/mol) in the polymer backbone.[13]

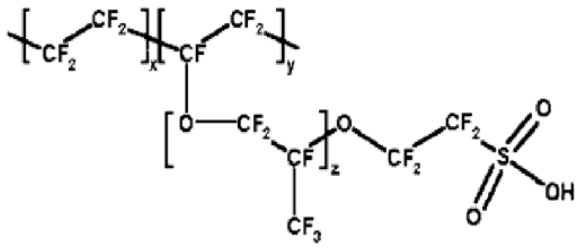

Figure 1. 2: Chemical structure of Nafion. Adapted from reference (14)

The conductivity of Nafion membranes relates to its morphology and has been widely discussed in the literature. Nafion phase segregates into distinct hydrophilic and hydrophobic regions. The hydrophilic regions contain sulfonate groups, swell and change size and shape with water uptake, creating a continuous network to allow water and ion transport efficiently. According to literature morphology of Nafion has clusters of sulfonate-ended perfluoroalkyl ether groups assembled as inverted micelles organized on a lattice as depicted in figure 3. These micelles are joined by channels which allow ion-hopping of positively charged species.[14]

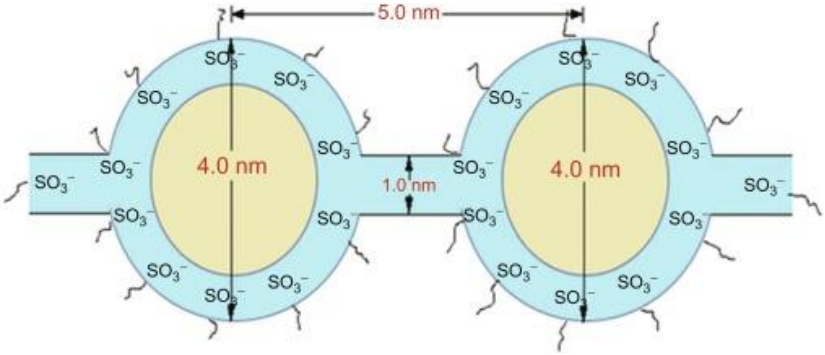

Figure 1. 3: Schematic illustration of the cluster-network interaction of water with the membrane. Adapted from reference (14)

However, despite its high ion conductivity and robust mechanical properties proton exchange membranes including Nafion has some well-known drawbacks. The main disadvantage is due to the operating acidic environment of PEM fuel cells require the use of precious metal-based catalysts such as platinum which increases the cost drastically and there's a concern that commercialization would be obstructed by inadequate platinum supply.[15] For any metal to be appropriate as an electrocatalyst in a fuel cell, it must not only have satisfactory catalytic activity and selectivity but must be also able to resist the rough chemical environment within the fuel cell. The presence of strong oxidants, low pH, reactive radicals, potential fluctuations high temperatures

limits the use of most transition metals in their pure form. Most dissolve at high electrode potentials and acidic environments.[16]

Apart from this PEM fuel cells limits the use of different fuels such as ammonia and hydrazine narrowing down its use. Even if ammonia is present in trace amounts as low as 1 ppm it could poison the PEMFCs by converting protons to NH_4^+ lowering the conductivity. Apart from this, it could particularly react with the anode catalyst layer, which carries ionomer in protonic form inhibiting hydrogen oxidation. Also, NH_3 could cross over to the cathode hindering the O2 reduction reaction as well.[17]

The other well-known drawback of the PEM fuel cells is that the limitations in using concentrated fuels as both protons and water moves in the same direction. However, even with these disadvantages PEM fuel cells still remains as the leading technology in the field but much attention is drawn towards the development of cost-effective anion exchange membranes as an alternative recently.

1.2.1 Anion exchange membrane fuel cells

Anion exchange membrane (AEM) research is fundamentally driven by the necessity to develop competent AEMs for anion exchange membrane water electrolysis and anion exchange membrane fuel cells operated in high pH and high-temperature environments. In the past 15 years, researches are motivated to expand the AEM technology complementary to PEMs to suit the needs of the above-mentioned applications mainly because of the cost associated with the PEM fuel cells.

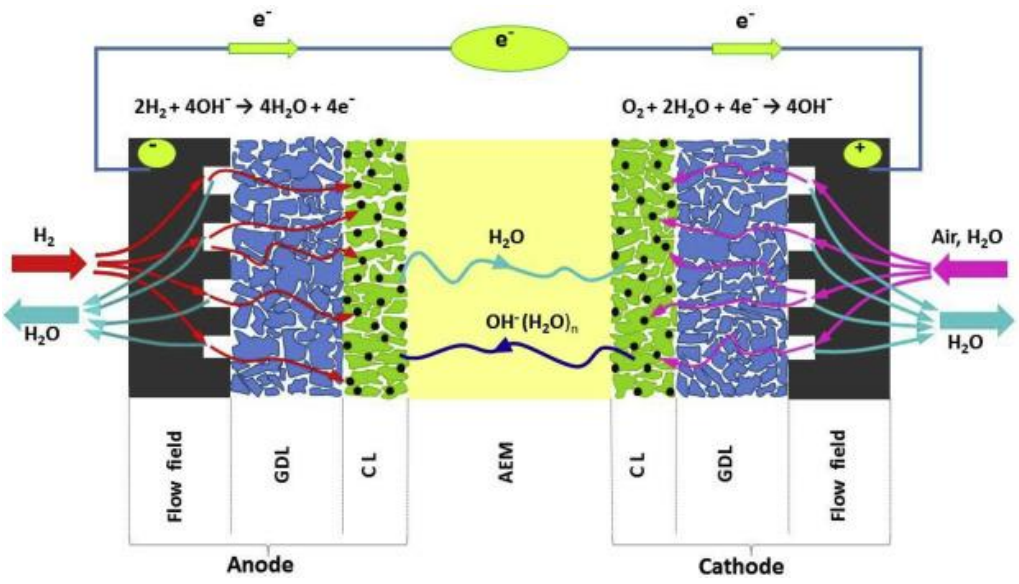

Figure 1. 4: Cell performance of an anion exchange membrane fuel cell. Adapted from reference (17)

When considering the electrode assembly gas diffusion layer (GDL) and the catalyst layer (CL) plays a vital role in maintaining the efficiency of a fuel cell. Basically, the gas diffusion layer is a porous material composed of a dense array of carbon fibers with high electrical and chemical conductivity and high chemical resistance towards corrosion. The key function of the gas diffusion layer is to manage the proper flow of reactant gasses (H_2 and O_2) and control the water management by removing water outside of the catalyst layer to prevent flooding and absorbing a certain quantity of water to help conductivity through the membrane. Catalyst layer functions to increase the reactive surface area significantly to enhance the oxidation-reduction kinetics.[18]

In an AEMFC H_2 or the fuel is charged to the anode and oxygen and water is charged to the cathode. Fuel is oxidized at the anode and combines with hydroxide ions transported from the cathode through the electrolyte (AEM) to form water. Part of the water exits the cell while the rest is transported through the electrolyte to the cathode. There, it is fused with oxygen and electrons

coming from the anode through an external circuit forming hydroxide ions that are then moved through the electrolyte to the anode. The electrochemical reactions are as follows.[19,20]

Cathode reaction: $O_2 + 2H_2O + 4e^- \longrightarrow 4OH^-$

Anode reaction: $2H_2 + 4OH^- \longrightarrow 4H_2O + 4e^-$

Overall reaction: $2H_2 + O_2 \longrightarrow 2H_2O$

Traditionally the same concept was used in alkaline fuel cells which used a liquid electrolyte (such as KOH) as the ion-conducting material before AEMFCs came into being. Even though much high ion conductivities have been reported they possessed an inherent error due to the formation of carbonate precipitates. When air containing CO_2 impurities enter the fuel cell it reacts with water or OH^- to produce carbonates as follows.

$CO_2 + OH^- \rightleftharpoons HCO_3^-$

$HCO^{3-} + OH^- \rightleftharpoons CO_3^{2-} + OH^-$

These carbonates react with K^+ coming from the electrolyte or Mg^{2+} or Ca^{2+} impurities forming insoluble precipitates reducing the performance of the fuel cell.[21,22]

As a remedy to this research was done on solid electrolytes which finally ended up developing polymer anion exchange membranes where the cation head group is immobilized in the polymer network minimizing its exposure to CO_2. In addition to this benefit, AEMs have many benefits over PEM fuel cell technology making it a better candidate against PEM fuel cells.

Predominantly AEMFCs are operated at an alkaline environment which allows the use of Pt-free catalysts which is critical to reducing the cost. In AEMFCs the high pH environment enables higher flexibility in choosing a non-precious metal-oriented catalyst. Transformation to the

alkaline environment widens the material space to architect a Pt-free electrocatalyst for oxidation and reduction reactions.[15] Nickel/nickel-metal alloys, silver electrocatalysts are two of many such catalysts widely used in AEMFCs.

The other advantage of AEMFCs is the alkaline environment permits the use of a variety of fuels including N based fuels such as ammonia and hydrazine. Unlike in PEM fuel cells, high pH surrounding improves electro-oxidation kinetics allowing the use of a greater variety of fuels other than H_2 and other low carbon-containing fuels. Also, it allows the use of more concentrated fuels. In AEMFCs water is both a reactant and a byproduct. Water is fed into the cell from the cathode side and also produced in the anode side. As a result of this water is transported through the cell via two mechanisms; electro-osmotic drag from the anode to the cathode with OH^- and back diffused to the anode side due to concentration gradient to institute equilibrium. Therefore, in contrast to PEM fuel cells in AEM fuel cells, water and ions move in the opposite directions facilitating the use of concentrated fuels.[23]

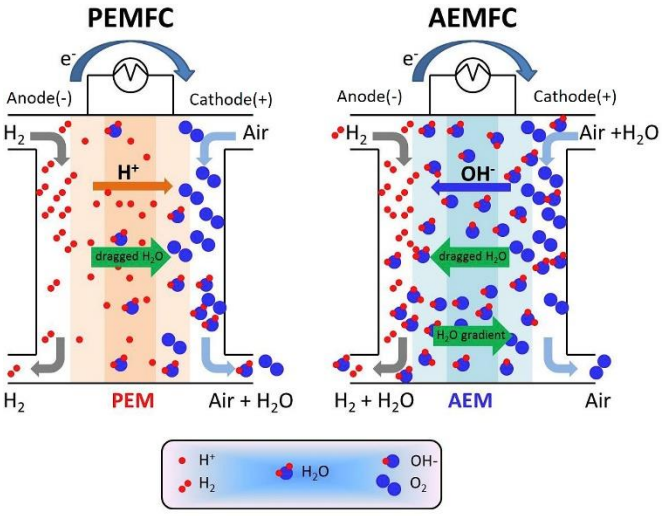

Figure 1. 5: The transport of ions and water in a PEMFC and an AEMFC. Adapted from reference (23)

Although AEMFCs have various promising advantages compared to PEMFCs there are two main issues still left to be addressed.

(1) The first issue associated with the AEMFCs is the low ion conductivity compared to proton conductivity in PEMFCs. This is mainly due to the large size of OH^- compared to protons leading to a high energy barrier for the transport of OH^- through the membrane. The most anion conductivities reported so far for the anion exchange membranes lies between 5 – 20 mS/cm.[24]

(2) The other issue is the lack of chemical and mechanical stability at high pH and elevated temperatures.[25,26]

Therefore AEM research is a hot research area driven by the need to develop cost-effective AEMs with high ion conductivity and high chemical and mechanical stability which can withstand harsh pH and temperature conditions.

Hence, the goal of this Master's dissertation is to address the aforementioned difficulties in anion exchange membrane fuel cells by synthesis and modification of an anion exchange membrane with high ion conductivity and high chemical and mechanical stability. Furthermore, this will give an insight into the effect of alignment via liquid crystalline properties to the conductivity.

1.3 Summary/ Overview of Dissertation

Currently, to deal with the global energy crisis and environmental concerns, greener technologies such as fuel cells and water electrolysis has drawn both industrial and academic attention. Among all eco- friendly technologies out there PEMFCs have known to be the most promising due to their high energy conversion efficiency, zero CO_2 emission and high power density regardless of it's dependence on precious- metal catalysts such as Pt. However commercialization of PEMFC technology has been greatly limited especially in developing countries due to its enormous initial cost. Therefore the escalation of AEMFC research is a promising alternative to the crucial cost barrier in utilizing fuel cells in large scale

Chapter 1 provides an insight into the significance of this study and an introduction to fuel cell technology. This chapter also highlights the fundamentals of both PEMFCs and AEMFCs, the electrochemical reactions and their pros and cons with respect to one another. Furthermore, this explains the importance of the development of cost-effective, highly efficient fuel cell technology to address the global energy crisis as well as environmental issues providing a concrete foundation to the further work that will be presented in this dissertation.

Chapter 2 describes the current state of the AEM technology and the remaining challenges. Here we discuss all the modifications and development done in fabricating an efficient anion exchange membrane and points out the shortcomings of the present fabrications to narrow down the developments needed to be done to address the aforementioned issues.

Chapter 3 explains the synthesis, characterization, and modification of a liquid crystalline brush like imidazolium copolymer membrane with higher ion conductivity and higher chemical and mechanical stability. There is no much research evidence for incorporating liquid crystalline

properties to enhance the conductivity and thus, this work will give an idea on the effect of alignment to the conductivity.

Finally, Chapter 4 describes the work in progress and future work in line to fabricate a polymer architecture with enhanced conductivity and stability as an alternative to high-cost PEMFCs.

1.4 References

(1) Zou, C.; Zhao, Q.; Zhang, G.; Xiong, B. Energy Revolution: From a Fossil Energy Era to a New Energy Era. *Nat. Gas Ind.* **2016**, *36* (1), 1–10. https://doi.org/10.3787/j.issn.1000-0976.2016.01.001.

(2) Pathak, S. Energy Crisis: A Review. *J. Eng. Res. Appl. www.ijera.com* **2014**, *4* (3), 845–851.

(3) Williams, R. G.; Roussenov, V.; Goodwin, P.; Resplandy, L.; Bopp, L. Sensitivity of Global Warming to Carbon Emissions: Effects of Heat and Carbon Uptake in a Suite of Earth System Models. *J. Clim.* **2017**, *30* (23), 9343–9363. https://doi.org/10.1175/JCLI-D-16-0468.1.

(4) Wang, S.; Jiang, S. P. Prospects of Fuel Cell Technologies. *Natl. Sci. Rev.* **2017**, nww099. https://doi.org/10.1093/nsr/nww099.

(5) Appleby, A. J. Fuel Cells and Hydrogen Fuel. *Int. J. Hydrogen Energy* **1994**, *19* (2), 175–180. https://doi.org/10.1016/0360-3199(94)90124-4.

(6) Kirubakaran, A.; Jain, S.; Nema, R. K. A Review on Fuel Cell Technologies and Power Electronic Interface. *Renewable and Sustainable Energy Reviews*. 2009, pp 2430–2440. https://doi.org/10.1016/j.rser.2009.04.004.

(7) Boudghene Stambouli, A.; Traversa, E. Fuel Cells, an Alternative to Standard Sources of Energy. *Renew. Sustain. Energy Rev.* **2002**, *6* (3), 295–304. https://doi.org/10.1016/S1364-0321(01)00015-6.

(8) Cook, B. Introduction to Fuel Cells and Hydrogen Technology. *Eng. Sci. Educ. J.* **2005**, *11* (6), 205–216. https://doi.org/10.1049/esej:20020601.

(9) Peighambardoust, S. J.; Rowshanzamir, S.; Amjadi, M. Review of the Proton Exchange Membranes for Fuel Cell Applications. In *International Journal of Hydrogen Energy*; 2010; Vol. 35, pp 9349–9384. https://doi.org/10.1016/j.ijhydene.2010.05.017.

(10) Xu, T. Ion Exchange Membranes: State of Their Development and Perspective. *Journal of Membrane Science*. 2005, pp 1–29. https://doi.org/10.1016/j.memsci.2005.05.002.

(11) Sone, Y. Proton Conductivity of Nafion 117 as Measured by a Four-Electrode AC Impedance Method. *J. Electrochem. Soc.* **2006**, *143* (4), 1254. https://doi.org/10.1149/1.1836625.

(12) Mauritz, K. A.; Moore, R. B. State of Understanding of Nafion. *Chem. Rev.* **2004**, *104* (10), 4535–4586. https://doi.org/10.1021/cr0207123.

(13) O'Hagan, D. Understanding Organofluorine Chemistry. An Introduction to the C-F Bond. *Chem. Soc. Rev.* **2008**, *37* (2), 308–319. https://doi.org/10.1039/b711844a.

(14) Sahu, A. K.; Pitchumani, S.; Sridhar, P.; Shukla, A. K. Nafion and Modified-Nafion Membranes for Polymer Electrolyte Fuel Cells: An Overview. *Bull. Mater. Sci.* **2009**, *32* (3), 285–294. https://doi.org/10.1007/s12034-009-0042-8.

(15) She, Z. W.; Kibsgaard, J.; Dickens, C. F.; Chorkendorff, I.; Nørskov, J. K.; Jaramillo, T. F. Combining Theory and Experiment in Electrocatalysis: Insights into Materials Design. *Science*. 2017. https://doi.org/10.1126/science.aad4998.

(16) Holton, O. T.; Stevenson, J. W. The Role of Platinum in Proton Exchange Membrane Fuel Cells. *Platinum Metals Review*. 2013, pp 259–271. https://doi.org/10.1595/147106713X671222.

(17) Uribe, F. A.; Gottesfeld, S.; Zawodzinski, T. A. Effect of Ammonia as Potential Fuel Impurity on Proton Exchange Membrane Fuel Cell Performance. *J. Electrochem. Soc.* **2002**, *149* (3), A293. https://doi.org/10.1149/1.1447221.

(18) Dekel, D. R. Review of Cell Performance in Anion Exchange Membrane Fuel Cells. *J. Power Sources* **2018**, *375*, 158–169. https://doi.org/10.1016/j.jpowsour.2017.07.117.

(19) Ramírez, S. C.; Paz, R. R. Hydroxide Transport in Anion-Exchange Membranes for Alkaline Fuel Cells. In *New Trends in Ion Exchange Studies*; 2018. https://doi.org/10.5772/intechopen.77148.

(20) Dekel, D. R. Review of Cell Performance in Anion Exchange Membrane Fuel Cells. *J. Power Sources* **2018**. https://doi.org/10.1016/j.jpowsour.2017.07.117.

(21) Zeng, K.; Zhang, D. Recent Progress in Alkaline Water Electrolysis for Hydrogen Production and Applications. *Progress in Energy and Combustion Science*. 2010, pp 307–326. https://doi.org/10.1016/j.pecs.2009.11.002.

(22) Ayers, K. E.; Anderson, E. B.; Capuano, C.; Carter, B.; Dalton, L.; Hanlon, G.; Manco, J.; Niedzwiecki, M. Research Advances towards Low Cost, High Efficiency PEM Electrolysis; 2010; pp 3–15. https://doi.org/10.1149/1.3484496.

(23) Varcoe, J. R.; Atanassov, P.; Dekel, D. R.; Herring, A. M.; Hickner, M. A.; Kohl, P. A.; Kucernak, A. R.; Mustain, W. E.; Nijmeijer, K.; Scott, K.; et al. Anion-Exchange Membranes in Electrochemical Energy Systems. *Energy and Environmental Science*. 2014, pp 3135–3191. https://doi.org/10.1039/c4ee01303d.

(24) Zheng, Y.; Ash, U.; Pandey, R. P.; Ozioko, A. G.; Ponce-González, J.; Handl, M.; Weissbach, T.; Varcoe, J. R.; Holdcroft, S.; Liberatore, M. W.; et al. Water Uptake Study of Anion Exchange Membranes. *Macromolecules* **2018**, *51* (9), 3264–3278. https://doi.org/10.1021/acs.macromol.8b00034.

(25) Li, Z.; He, X.; Jiang, Z.; Yin, Y.; Zhang, B.; He, G.; Tong, Z.; Wu, H.; Jiao, K. Enhancing Hydroxide Conductivity and Stability of Anion Exchange Membrane by Blending Quaternary Ammonium Functionalized Polymers. *Electrochim. Acta* **2017**, *240*, 486–494. https://doi.org/10.1016/j.electacta.2017.04.109.

(26) Gottesfeld, S.; Dekel, D. R.; Page, M.; Bae, C.; Yan, Y.; Zelenay, P.; Kim, Y. S. Anion Exchange Membrane Fuel Cells: Current Status and Remaining Challenges. *J. Power Sources* **2018**, *375*, 170–184. https://doi.org/10.1016/j.jpowsour.2017.08.010.

Chapter 2 - Anion exchange membranes – current status and remaining challenges

2.1 Introduction

To guarantee high power density, long term operation and practical applications of the cell anion exchange membranes (AEM) should posses high ion conductivity, superior chemical and mechanical stability, cost-effectiveness and easy synthesis pathways. In the pursuit of advancing AEMs with above-mentioned characteristics, numerous challenges in both materials and technology have been encountered. To address these issues research has aimed at two main areas in the past ten years. (1) Develop the ion exchanging head group to improve ion conductivity and the (2) fabricate a new polymer architecture with high chemical and mechanical stability and improved ion conductivity.

2.2 Advancements in the anion exchange head groups

In general anion exchange head groups can be dived into two main categories: (1) Nitrogen(N) containing head groups and (2)N-free head groups. Nitrogen-containing head groups include quaternary ammonium ions, imidazolium, pyridinium and guanidinium based head groups while N-free head groups consist of sulphonium, phosphonium and methyl cations such as ruthenium and nickel. Conventionally anion exchange membrane head groups have been quaternary ammonium ions due to their relatively easy synthesis methods, good conductivity, and stability. For example, AEMs with quaternary ammonium ions could be simply synthesized by reacting a polymer containing a benzyl halide with an amine such as triethylamine to introduce an ammonia group and then it could be converted to the salt form by treating with a base like KOH.(Menshutkin reaction, Figure 2.1)[1,2].

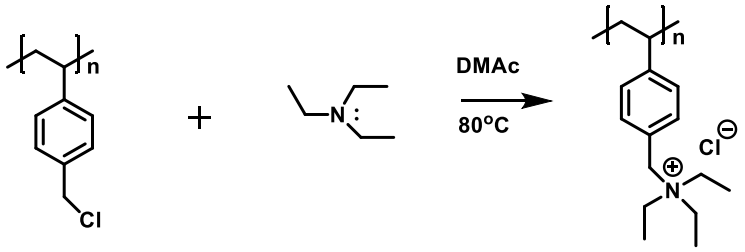

Figure 2. 1: Reaction of triethylamine with benzyl chloride

In comparison to quaternary phosphoniums and quaternary sulphonium, quaternary ammoniums have shown high conductivity and stability.[3,4] The main reason behind this is amines used in the synthesis (specifically diamines) act as both quaternization and crosslinking agents.[5] DABCO (1,4-diazabicyclo[2,2,2]octane) and TMHDA (N, N, N, N-tetramethylhexane diammonium) are two well known tertiary diamine head groups.[6] Self-crosslinking ability is vital since it enhances mechanical properties and simplifies the membrane preparation by cutting down one step. For example, two N atoms present in DABCO makes it an adaptable structure to be tied through two positions enabling the self-crosslinking.

Despite these advantages, quaternary ammonium containing AEMs have one major drawback which leads to membrane degradation. The quaternary ammonium group is susceptible to OH^- attack which leads to the degradation of NH_4^+ finally resulting in low ion conductivity. This happens mainly via Hoffmann elimination and nucleophilic substitution reactions[5](Figure 2.2).

To overcome this problem, research has focused on introducing large functional groups such as phenyl groups to block the cation site and thereby prevent the attack of OH^-. Also by introducing electron-donating groups such as methoxy groups hydroxide attacks could be minimized to a satisfactory level.

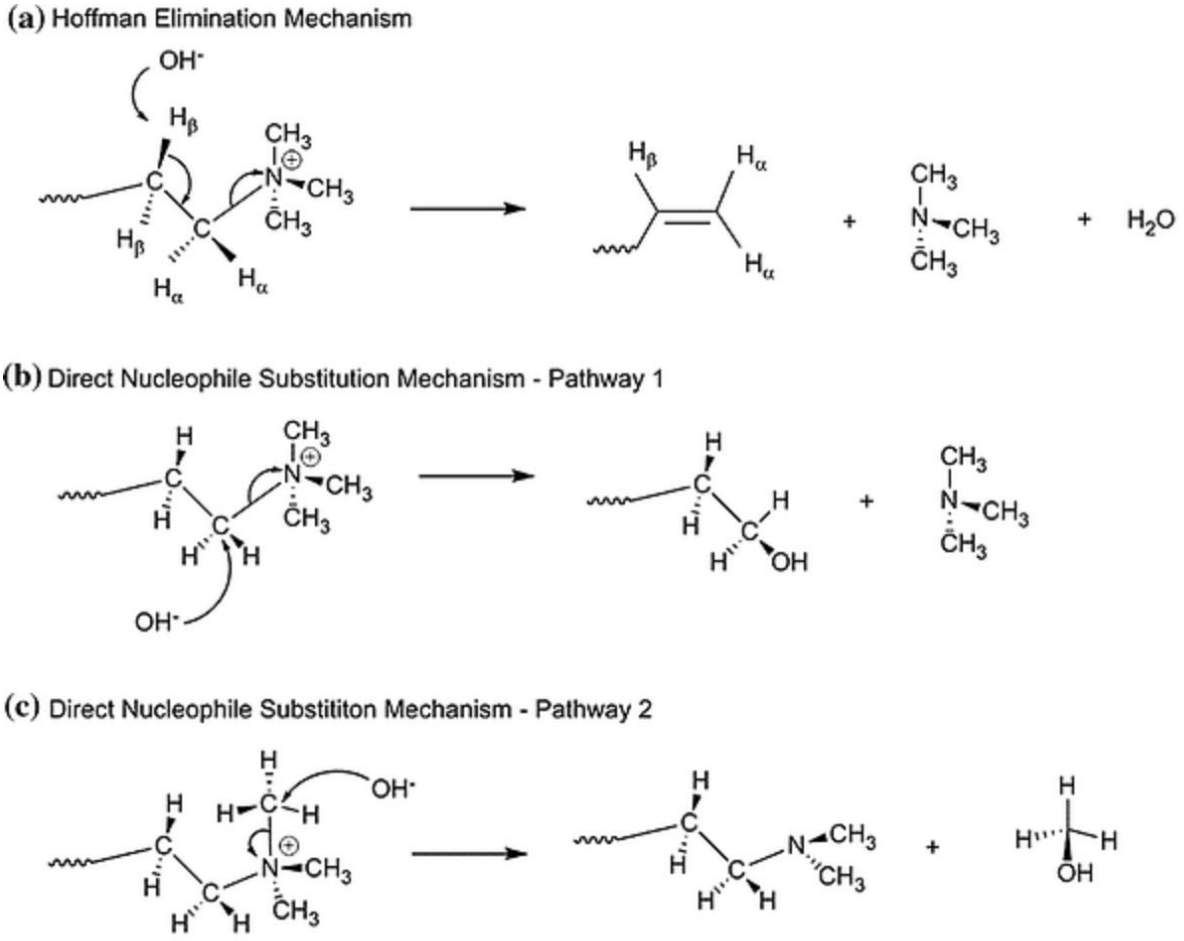

Figure 2. 2: Degradation mechanisms for quaternary ammonium ions. Adapted from reference (5)

With this understanding, researchers have revised the use of phosphonium and sulfonium ions because they also face the same degradability issue as quaternary ammonium ion containing AEMs. Some have postulated that phosphonium and sulphonium based AEMs could be synthesized in similar methods to quaternary ammonium ion-based AEMs by addition of phenyl groups to introduce steric hinderance and electron-donating methoxy groups to make the cation center less positive. However this work is relatively recent and further research has to be done to

synthesize N-free membranes to match or exceed the performance of quaternary ammonium-based AEMs.[7,8,9]

In addition to the aforementioned modifications, investigations have been largely done on developing AEMs with other N containing head groups such as imidazolium, pyridinium and guanidium. Among these imidazolium-based AEMs have gained the greatest attention due to its adaptable chemical structure, easy synthesis methods and selective solubilities in some of the water-miscible solvents. Imidazole functionalized membranes do not dissolve in alcohols or their aqueous solutions but dissolve in low boiling point solvents such as tetrahydrofuran. This unique solubility of imidazole allows imidazolium functionalized AEMs to be used in alcohol fuel cells.[10,11]

Among the many imidazolium-based AEMs, platforms containing with benzimidazolium head groups have shown highest and closest ion conductivity to that of traditional quaternary ammonium-based AEMs. This is mainly due to the conjugate resonance observed between the imidazolium ring and the phenyl group and the ion cluster formation ability. Therefore imidazolium head groups containing AEM is a competitive candidate worth doing additional research.[12,13]

Despite all these advantages, imidazolium functionalized AEMs also comes with an inherent drawback. Multiple research articles have highlighted the chance of a nucleophilic attack on electron-deficient C2 position which results in ring-opening leading to degradation of the membrane with time.[10] However, research on stabilizing the imidazolium cation has postulated that stability could be obtained by reversible deprotonation reactions accompanied by stabilizing the C2 position by steric effects and resonance. Also it has been indicated that imidazolium head groups with H at the C2 position are more stable compared to those having larger electron-donating groups at the C2 position conflicting with the prior postulation(Figure 3.2)[14]. Clear evidence on this as to whether having a bulky group on C2 position stabilizes the cation or whether it destabilize the structure further has not yet been published.

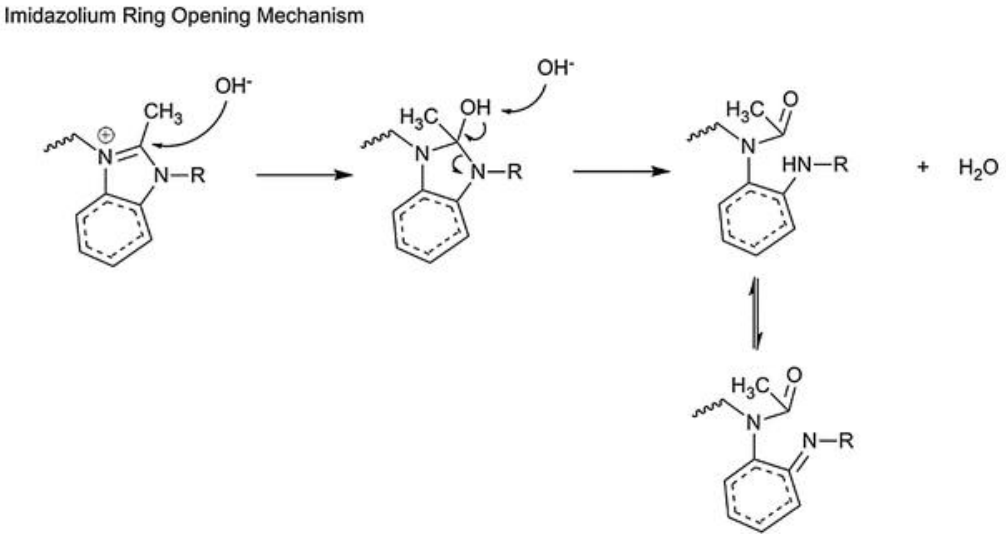

Figure 2. 3: Immadozolium degradation mechanism. Adapted from reference (5)

The final category of N-free head groups includes metal cations such as Ni, Ru, and Co. The significance of using metals as the anion exchanging site is that divalent cations could be introduced to the membrane which can accommodate two anions per site. The first-ever metal-based AEM was synthesized using Ruthenium challenging all the other monovalent AEMs synthesized so far. But still the metal-based AEMs are under research and it could be one possible path that could address the low mobility of OH^- compared to protons. [15,16]

In conclusion, there is no such anion exchanging head group considered as the "best" and all have their inherent pros and cons. Nevertheless, literature has highlighted some promising ion exchanging head groups such as imidazole that are worthy of further studying.

2.3 Advancements in the polymer architecture

Designing polymer architecture to improve ion conductivity and stability is equally important as developing new ion exchanging head group. One could simply postulate that by increasing the ion exchanging sites ion exchanging capacity could be improved. But as the number of ion exchanging sites increases the water uptake increases leading to membrane swelling which finally results in membrane degradation. The stability lost due to this could be improved by increasing the crosslinking percentage but this lowers the mobility of ions resulting in low ion conductivity. Therefore, there's a fine line between increasing the number of exchanging sites, percent crosslinking and the stability of the membrane. Thus we will focus on fabrication of proper polymer architectures which could fill the missing parts of this puzzle.

This could be addressed via two main approaches. First, by improving the main chain chemistry and then improving the side chain chemistry.

2.3.1 Advancements in main-chain/backbone chemistry

According to literature most widely used backbones are polysulfones, polyether ketones, polybenzimidazole, poly(2,6-dimethyl-1,4-phenylene oxide) (PPO) and poly(vinylidene fluoride) either due to their ability to withstand harsh conditions and their ability to undergo further synthetic modifications. For instance, polysulfone is a thermoplastic material that is soluble in many organic solvents and contains two activated sites per repeating unit that are susceptible to electrophilic substitution. This provides significantly high degrees of functionalization[17]. Similarly, polyfluorones are significant in AEMs due to their unique physical properties, ability to undergo a variety of functionalizations with extended conjugations, excellent film-forming properties and high chemical stability in high pH environments due to the absence of aryl ether ketones.[18,19]

But these backbones are also subjected to backbone degradation. Polysulfones can be easily hydrolyzed at alkaline environments due to the presence of the ether group and polyfluorenes are prone to dehydrofluorination as follows.[20,21, 22,23].Also backbones with quaternary carbons also should be avoided since they also can undergo hydrolysis degrading the membranes over time.

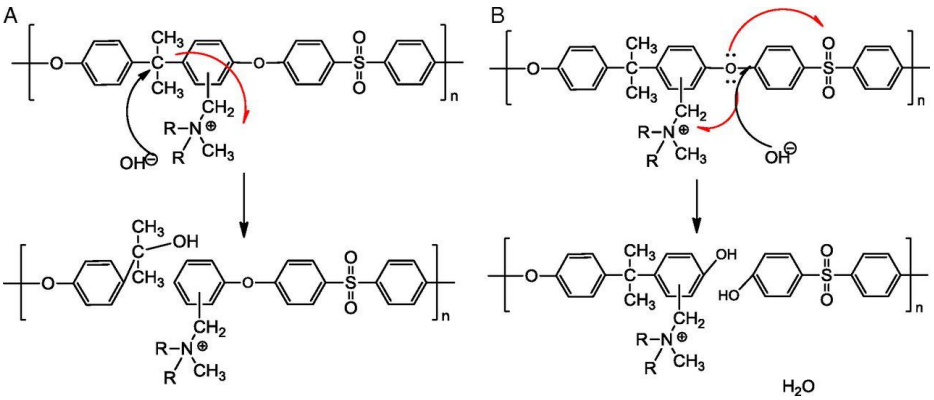

Figure 2. 4: The degradation mechanisms of (A) quaternary carbon and (B) ether bonds in polysulfones

As discussed above apart from the alkaline degradation of the anion exchanging sites membrane stability is also affected by the polymer backbone degradation and therefore research attention is highly focused on fabricating polymer backbone architectures susceptible to hydrolysis and degradation. While searching for a polymer backbone with these characteristics polynorbornene has shown promising features making it a competitive candidate in the AEM industry.[24]

Polynorbonene is an interesting polymer backbone candidate for AEMs since it could be modified in numerous ways chemically to synthesis different types of monomers. Norbornene can be polymerized via ring-opening metathesis polymerization (ROMP) and vinyl addition polymerization. In addition to these norbornene exhibits excellent film-forming properties and ability to crosslinks, which results in tunable mechanical properties and chemical stability of the membrane. Literature highlights a number of AEMs with polynorbornene where conductivities as high as 18 mS/cm has observed at 20˚ C.[25]

2.3.2 Advancements in the side chain polymers

The main obstruction for the commercialization of the AEMFCs is the poor hydroxide conductivity of the AEM. In parallel to improving the conductivity via developing the anion exchanging head group interesting work has been revealed on enhancing the conductivity via designing the rational polymer architecture. Prior studies have manifested that main chain type AEMs where the cationic head group is fixed via short linkages such as CH_2 do not display a satisfactory conductivity and that by having the cation head group attached to regularly spaced flexible side chains high anion conductivity could be obtained (Figure 2.5)[26].

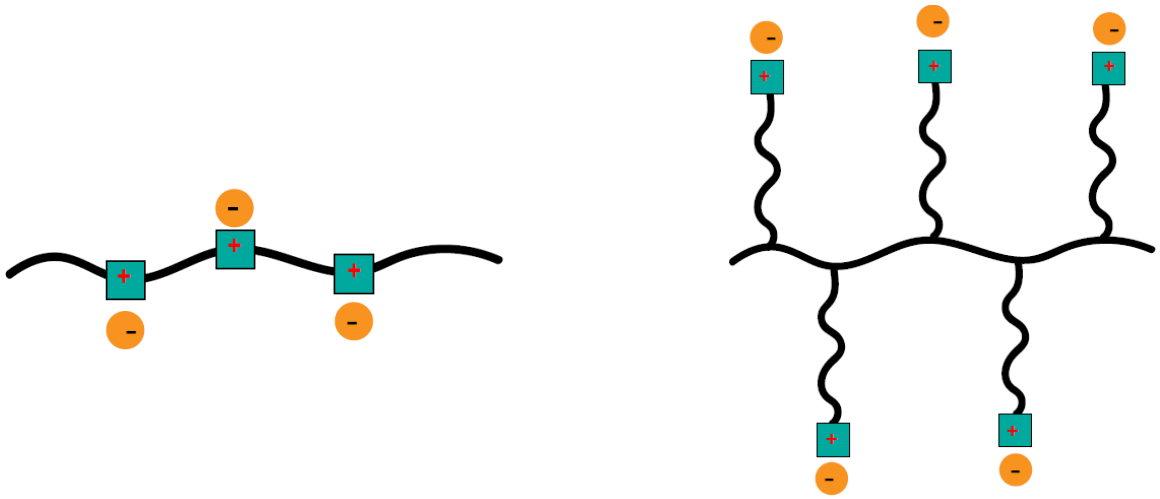

Figure 2. 5: Schematic illustration of a main chain polymer architecture vs side-chain polymer architecture

In principle lengthening the spacer group should improve the conductivity by supporting the formation of highly ordered phase-separated morphology. This distinct phase separation occurs due to the enthalpy related to the demixing of the hydrophobic polymer backbone with the hydrophilic ionic side chains. These side chains or pendant groups self assemble to create hydrophilic channels where OH- is transported via Grotthus type mechanism. Still, the transport mechanism of hydroxide ions through the membrane is not understood precisely but several postulations have been made and most of them agree with the grotthus type ion hopping mechanism (Figure 2.6). Hydroxide ions hydrogen bond with the water molecules to construct different hydration complexes and these solvated hydroxide ions move through the ionic channels as a result of electro-osmotic drag or the concentration gradient. [27]

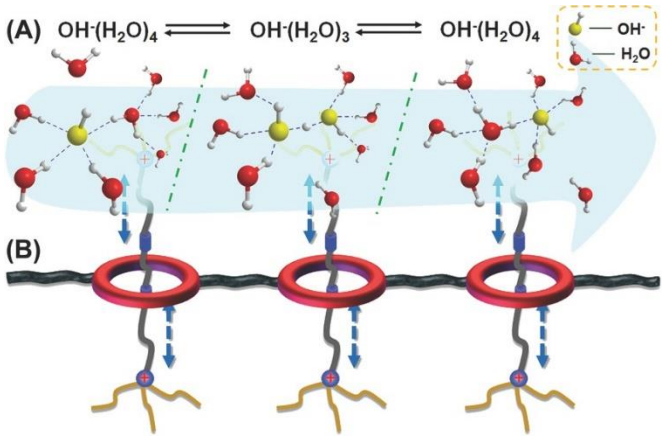

Figure 2. 6: Schematic illustration of (A) Transportation of hydroxide ions via the formation of hydration complexes. (B) A cartoon of how ion channels are located in a comb-shaped polymer architecture. Adapted from reference (27)

The ionic channels formed due to the phase segregation contain highly flexible pendant groups having the cation head group attached at the end. This flexibility allows it to make interactions with the hydrated ions more efficiently than the hydrophobic rigid backbone. Even though ionic conductivity could be improved by increasing the number of ion exchange sites it could lead to excessive membrane swelling. However by the above-mentioned polymer architectural difference, though some amount of dimensional swelling is observed it is not as excessive as the swelling observed by increasing the number of ion-exchange sites. Over the past ten years, multiple strategies have been introduced aiming to enhance conductivity via phase separation and one striking strategy guaranteed AEMs with high ion conductivity is to develop a polymer containing hydrophobic main chain and hydrophilic regularly spaced flexible side chains. [28]

2.3.3 Advancements in the polymer architecture and composition – effect of homopolymers, block copolymers and random copolymers

As discussed in the previous section morphology, domain size and orientation have a high impact on developing the conductivity and stability of an AEM. For instance, Nafion exhibits a domain size of 10-12 nm it has been experimentally proven that it leads for higher conductivity and stability. The type of polymer design, that is a homopolymer, block and random copolymer architectures play an important role in determining the microstructure and phase separation of a polymer. A number of studies have demonstrated that the block copolymer architecture shows a significant increase in ion conductivity compared to their analogous homopolymers and random copolymers proposing that confinement of ionic groups in block copolymers help in creating nanostructures containing localized ion concentrations.[29]

By definition, block copolymers are macromolecular amphiphiles made of chemically distinct blocks of homopolymers. The enthalpy of demixing of diverse polymer segments result in the formation of microdomains and the physical interconnection of the blocks limit the phase segregation to occur only on length scales equivalent to the radius of gyration of the polymer. The degree of phase separation depends on the volume fraction of the components (Figure 2.7).[30]

Based on the degree of polymerization and segregation robustness block copolymers proceeds to polymer architectures with well microphase separated, nanostructured membranes with various morphologies (Figure 2.7).

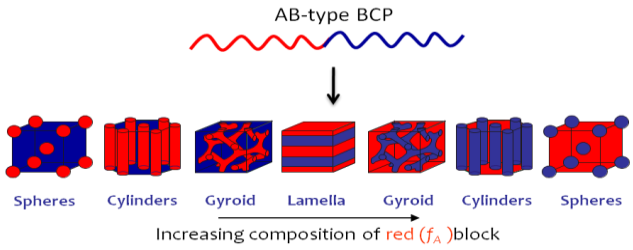

Figure 2. 7: Schematic illustration of a melt state phase behavior of a diblock copolymer

The morphology – ion transport relationship in block copolymers advances the conductivity in several magnitudes compared to random copolymers(Figure 2.8). For example in a study where the conductivity of block and random architectures of Poly(arylene ether sulfone) having the same ion exchange capacity (1.6 meq/g) was measured, block copolymer reported a conductivity of 21.37 mS/cm while the random copolymer showed a lesser conductivity (17.91 mS/cm) at 80˚ C and 100% relative humidity.[31,32,33]

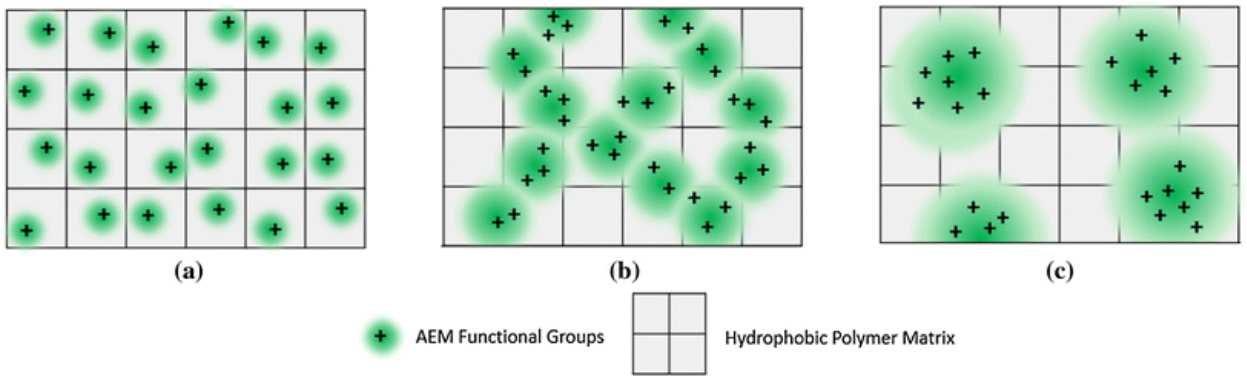

Figure 2. 8: Schematic illustration of the development of ion channels in AEM. (a) Dispersed and underdeveloped ion channels in homopolymers, (b)interconnected ion channels in random copolymers, (c)segregated overdeveloped ion channels with distinct hydrophilic/hydrophobic regions in block copolymers. Adapted from reference (32)

Another significant advantage of block copolymers is the ability to obtain well-defined polymer nanostructures with two or more blocks having tunable properties. The ionic block contributes to well defined perpetual hydrophilic channels which promote conductivity while the other blocks maintain the mechanical integrity.

2.4 The role of liquid crystals in AEMs

As discussed from the beginning of this chapter the biggest drawback of AEMs is their how hydroxide ion conductivity. To address this AEMs are generally designed with high ion exchange capacities but it comes with other expenses such as excessive membrane swelling and low mechanical integrity due to the increased number of ion exchanging sites.[35]

Therefore one promising approach towards the design of AEMs with high ion conductivity is to improve ionic mobility. The self-assembly of liquid crystalline polymers has been found to be a versatile approach in improving conductivity since they create highly ordered well-defined ionic channels. Liquid crystals (LCs) possess many of the physical characteristics of a liquid but the molecular units are sufficiently ordered to give rise to some anisotropy.

Although the incorporation of LCs to obtain ordered alignment of ionic clusters is still rather limited successful research has been reported on designing ion transporting self-assembled soft materials forming 1D[36], 2D[37] and 3D[38] ionic pathways. Alignment of LCs could be achieved by electric fields and magnetic fields but the control of alignment is challenging in terms of scalability and stability of the polymer material (Figure 2.9)[39,40].

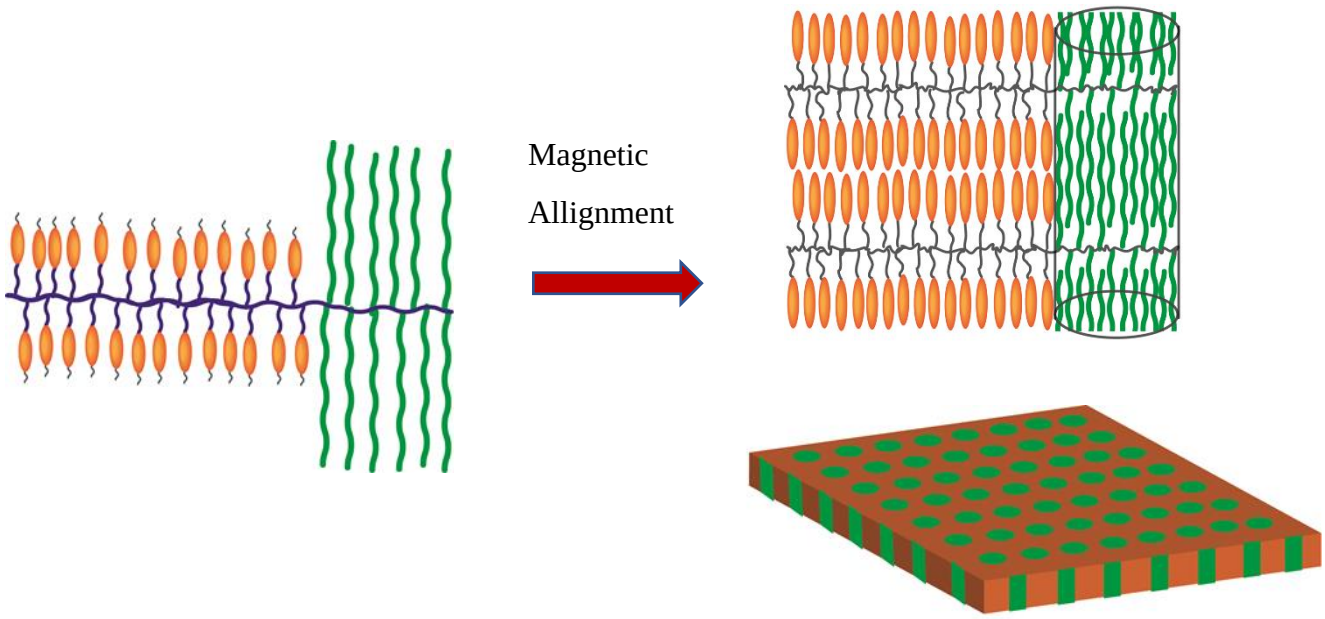

Figure 2. 9: Schematic illustration of self-assembly of a diblock copolymer containing LCs. Adapted from reference (40)

2.5 References

(1) Ariyanfar, L.; Ghadamian, H.; Roshandel, R. Alkaline Fuel Cell (AFC) Engineering Design, Modeling and Simulation for UPS Provide in Laboratory Application; 2011; pp 1227–1234. https://doi.org/10.3384/ecp110571227.

(2) Gottesfeld, S.; Dekel, D. R.; Page, M.; Bae, C.; Yan, Y.; Zelenay, P.; Kim, Y. S. Anion Exchange Membrane Fuel Cells: Current Status and Remaining Challenges. *J. Power Sources* **2018**, *375*, 170–184. https://doi.org/10.1016/j.jpowsour.2017.08.010.

(3) Ponce-González, J.; Whelligan, D. K.; Wang, L.; Bance-Soualhi, R.; Wang, Y.; Peng, Y.; Peng, H.; Apperley, D. C.; Sarode, H. N.; Pandey, T. P.; et al. High Performance Aliphatic-Heterocyclic Benzyl-Quaternary Ammonium Radiation-Grafted Anion-Exchange Membranes. *Energy Environ. Sci.* **2016**, *9* (12), 3724–3735. https://doi.org/10.1039/c6ee01958g.

(4) Varcoe, J. R.; Atanassov, P.; Dekel, D. R.; Herring, A. M.; Hickner, M. A.; Kohl, P. A.; Kucernak, A. R.; Mustain, W. E.; Nijmeijer, K.; Scott, K.; et al. Anion-Exchange Membranes in Electrochemical Energy Systems. *Energy and Environmental Science*. 2014, pp 3135–3191. https://doi.org/10.1039/c4ee01303d.

(5) Hagesteijn, K. F. L.; Jiang, S.; Ladewig, B. P. A Review of the Synthesis and Characterization of Anion Exchange Membranes. *Journal of Materials Science*. 2018, pp 11131–11150. https://doi.org/10.1007/s10853-018-2409-y.

(6) Wang, J.; He, G.; Wu, X.; Yan, X.; Zhang, Y.; Wang, Y.; Du, L. Crosslinked Poly (Ether Ether Ketone) Hydroxide Exchange Membranes with Improved Conductivity. *J. Memb. Sci.* **2014**, *459*, 86–95. https://doi.org/10.1016/j.memsci.2014.01.068.

(7) Gu, S.; Cai, R.; Yan, Y. Self-Crosslinking for Dimensionally Stable and Solvent-Resistant Quaternary Phosphonium Based Hydroxide Exchange Membranes. *Chem. Commun.* **2011**, *47* (10), 2856–2858. https://doi.org/10.1039/c0cc04335d.

(8) Zhang, B.; Gu, S.; Wang, J.; Liu, Y.; Herring, A. M.; Yan, Y. Tertiary Sulfonium as a Cationic Functional Group for Hydroxide Exchange Membranes. *RSC Adv.* **2012**, *2* (33), 12683–12685. https://doi.org/10.1039/c2ra21402d.

(9) Hossain, M. A.; Jang, H.; Sutradhar, S. C.; Ha, J.; Yoo, J.; Lee, C.; Lee, S.; Kim, W. Novel Hydroxide Conducting Sulfonium-Based Anion Exchange Membrane for Alkaline Fuel Cell Applications. In *International Journal of Hydrogen Energy*; 2016; Vol. 41, pp 10458–10465. https://doi.org/10.1016/j.ijhydene.2016.01.051.

(10) Wang, J.; Gu, S.; Kaspar, R. B.; Zhang, B.; Yan, Y. Stabilizing the Imidazolium Cation in Hydroxide-Exchange Membranes for Fuel Cells. *ChemSusChem* **2013**, *6* (11), 2079–2082. https://doi.org/10.1002/cssc.201300285.

(11) Li, Z.; Zhang, Y.; Cao, T.; Yang, Y.; Xiong, Y.; Xu, S.; Xu, Z. Highly Conductive Alkaline Anion Exchange Membrane Containing Imidazolium-Functionalized Octaphenyl

Polyhedral Oligomeric Silsesquioxane Filler. *J. Memb. Sci.* **2017**, *541*, 474–482. https://doi.org/10.1016/j.memsci.2017.07.037.

(12) Guo, D.; Lai, A. N.; Lin, C. X.; Zhang, Q. G.; Zhu, A. M.; Liu, Q. L. Imidazolium-Functionalized Poly(Arylene Ether Sulfone) Anion-Exchange Membranes Densely Grafted with Flexible Side Chains for Fuel Cells. *ACS Appl. Mater. Interfaces* **2016**, *8* (38), 25279–25288. https://doi.org/10.1021/acsami.6b07711.

(13) Lin, X.; Liang, X.; Poynton, S. D.; Varcoe, J. R.; Ong, A. L.; Ran, J.; Li, Y.; Li, Q.; Xu, T. Novel Alkaline Anion Exchange Membranes Containing Pendant Benzimidazolium Groups for Alkaline Fuel Cells. *J. Memb. Sci.* **2013**, *443*, 193–200. https://doi.org/10.1016/j.memsci.2013.04.059.

(14) Price, S. C.; Williams, K. S.; Beyer, F. L. Relationships between Structure and Alkaline Stability of Imidazolium Cations for Fuel Cell Membrane Applications. *ACS Macro Lett.* **2014**, *3* (2), 160–165. https://doi.org/10.1021/mz4005452.

(15) Zha, Y.; Disabb-Miller, M. L.; Johnson, Z. D.; Hickner, M. A.; Tew, G. N. Metal-Cation-Based Anion Exchange Membranes. *J. Am. Chem. Soc.* **2012**, *134* (10), 4493–4496. https://doi.org/10.1021/ja211365r.

(16) Kwasny, M. T.; Tew, G. N. Expanding Metal Cation Options in Polymeric Anion Exchange Membranes. *J. Mater. Chem. A* **2017**, *5* (4), 1400–1405. https://doi.org/10.1039/c6ta07990c.

(17) Teresa Pérez-Prior, M.; Ureña, N.; Tannenberg, M.; del Río, C.; Levenfeld, B. DABCO-Functionalized Polysulfones as Anion-Exchange Membranes for Fuel Cell Applications: Effect of Crosslinking. *J. Polym. Sci. Part B Polym. Phys.* **2017**, *55* (17), 1326–1336. https://doi.org/10.1002/polb.24390.

(18) Zhang, F.; Zhang, H.; Ren, J.; Qu, C. PTFE Based Composite Anion Exchange Membranes: Thermally Induced in Situ Polymerization and Direct Hydrazine Hydrate Fuel Cell Application. *J. Mater. Chem.* **2010**, *20* (37), 8139–8146. https://doi.org/10.1039/c0jm01311k.

(19) Lee, W. H.; Mohanty, A. D.; Bae, C. Fluorene-Based Hydroxide Ion Conducting Polymers for Chemically Stable Anion Exchange Membrane Fuel Cells. *ACS Macro Lett.* **2015**, *4* (4), 453–457. https://doi.org/10.1021/acsmacrolett.5b00145.

(20) Arges, C. G.; Ramani, V. Two-Dimensional NMR Spectroscopy Reveals Cation-Triggered Backbone Degradation in Polysulfone-Based Anion Exchange Membranes. *Proc. Natl. Acad. Sci.* **2013**, *110* (7), 2490–2495. https://doi.org/10.1073/pnas.1217215110.

(21) Nuñez, S. A.; Hickner, M. A. Quantitative 1H NMR Analysis of Chemical Stabilities in Anion-Exchange Membranes. *ACS Macro Lett.* **2013**, *2* (1), 49–52. https://doi.org/10.1021/mz300486h.

(22) Miyanishi, S.; Yamaguchi, T. Ether Cleavage-Triggered Degradation of Benzyl

Alkylammonium Cations for Polyethersulfone Anion Exchange Membranes. *Phys. Chem. Chem. Phys.* **2016**, *18* (17), 12009–12023. https://doi.org/10.1039/c6cp00579a.

(23) Sata, T.; Tsujimoto, M.; Yamaguchi, T.; Matsusaki, K. Change of Anion Exchange Membranes in an Aqueous Sodium Hydroxide Solution at High Temperature. *J. Memb. Sci.* **1996**, *112* (2), 161–170. https://doi.org/10.1016/0376-7388(95)00292-8.

(24) Chen, W.; Mandal, M.; Huang, G.; Wu, X.; He, G.; Kohl, P. A. Highly Conducting Anion-Exchange Membranes Based on Cross-Linked Poly(Norbornene): Ring Opening Metathesis Polymerization. *ACS Appl. Energy Mater.* **2019**, *2* (4), 2458–2468. https://doi.org/10.1021/acsaem.8b02052.

(25) Clark, T. J.; Robertson, N. J.; Kostalik IV, H. A.; Lobkovsky, E. B.; Mutolo, P. F.; Abruña, H. D.; Coates, G. W. A Ring-Opening Metathesis Polymerization Route to Alkaline Anion Exchange Membranes: Development of Hydroxide-Conducting Thin Films from an Ammonium-Functionalized Monomer. *J. Am. Chem. Soc.* **2009**, *131* (36), 12888–12889. https://doi.org/10.1021/ja905242r.

(26) Weiber, E. A.; Meis, D.; Jannasch, P. Anion Conducting Multiblock Poly(Arylene Ether Sulfone)s Containing Hydrophilic Segments Densely Functionalized with Quaternary Ammonium Groups. *Polym. Chem.* **2015**, *6* (11), 1986–1996. https://doi.org/10.1039/c4py01588f.

(27) Ge, X.; He, Y.; Guiver, M. D.; Wu, L.; Ran, J.; Yang, Z.; Xu, T. Alkaline Anion-Exchange Membranes Containing Mobile Ion Shuttles. *Adv. Mater.* **2016**, *28* (18), 3467–3472. https://doi.org/10.1002/adma.201506199.

(28) He, Y.; Si, J.; Wu, L.; Chen, S.; Zhu, Y.; Pan, J.; Ge, X.; Yang, Z.; Xu, T. Dual-Cation Comb-Shaped Anion Exchange Membranes: Structure, Morphology and Properties. *J. Memb. Sci.* **2016**, *515*, 189–195. https://doi.org/10.1016/j.memsci.2016.05.058.

(29) Tuli, S. K.; Roy, A. L.; Elgammal, R. A.; Tian, M.; Zawodzinski, T. A.; Fujiwara, T. Effect of Morphology on Anion Conductive Properties in Self-Assembled Polystyrene-Based Copolymer Membranes. *J. Memb. Sci.* **2018**, *565*, 213–225. https://doi.org/10.1016/j.memsci.2018.08.028.

(30) Hu, H.; Gopinadhan, M.; Osuji, C. O. Directed Self-Assembly of Block Copolymers: A Tutorial Review of Strategies for Enabling Nanotechnology with Soft Matter. *Soft Matter*. 2014, pp 3867–3889. https://doi.org/10.1039/c3sm52607k.

(31) Chen, H.; Choi, J. H.; Cruz, D. S. D. La; Winey, K. I.; Elabd, Y. A. Polymerized Ionic Liquids: The Effect of Random Copolymer Composition on Ion Conduction. *Macromolecules* **2009**, *42* (13), 4809–4816. https://doi.org/10.1021/ma900713e.

(32) Hossain, M. A.; Lim, Y.; Lee, S.; Jang, H.; Choi, S.; Jeon, Y.; Lim, J.; Kim, W. G. Comparison of Alkaline Fuel Cell Membranes of Random & Block Poly(Arylene Ether Sulfone) Copolymers Containing Tetra Quaternary Ammonium Hydroxides. In *International Journal of Hydrogen Energy*; 2014.

https://doi.org/10.1016/j.ijhydene.2013.01.197.

(33) Pan, J.; Chen, C.; Li, Y.; Wang, L.; Tan, L.; Li, G.; Tang, X.; Xiao, L.; Lu, J.; Zhuang, L. Constructing Ionic Highway in Alkaline Polymer Electrolytes. *Energy Environ. Sci.* **2014**, *7* (1), 354–360. https://doi.org/10.1039/c3ee43275k.

(34) Hamley, I. W. Nanoshells and Nanotubes from Block Copolymers. *Soft Matter*. 2005, pp 36–43. https://doi.org/10.1039/b418226j.

(35) Hibbs, M. R.; Fujimoto, C. H.; Cornelius, C. J. Synthesis and Characterization of Poly(Phenylene)-Based Anion Exchange Membranes for Alkaline Fuel Cells. *Macromolecules* **2009**, *42* (21), 8316–8321. https://doi.org/10.1021/ma901538c.

(36) Yoshio, M.; Kagata, T.; Hoshino, K.; Mukai, T.; Ohno, H.; Kato, T. One-Dimensional Ion-Conductive Polymer Films: Alignment and Fixation of Ionic Channels Formed by Self-Organization of Polymerizable Columnar Liquid Crystals. *J. Am. Chem. Soc.* **2006**, *128* (16), 5570–5577. https://doi.org/10.1021/ja0606935.

(37) Hoshino, K.; Yoshio, M.; Mukai, T.; Kishimoto, K.; Ohno, H.; Kato, T. Nanostructured Ion-Conductive Films: Layered Assembly of a Side-Chain Liquid-Crystalline Polymer with an Imidazolium Ionic Moiety. In *Journal of Polymer Science, Part A: Polymer Chemistry*; 2003; Vol. 41, pp 3486–3492. https://doi.org/10.1002/pola.10832.

(38) Soberats, B.; Yoshio, M.; Ichikawa, T.; Taguchi, S.; Ohno, H.; Kato, T. 3D Anhydrous Proton-Transporting Nanochannels Formed by Self-Assembly of Liquid Crystals Composed of a Sulfobetaine and a Sulfonic Acid. *J. Am. Chem. Soc.* **2013**, *135* (41), 15286–15289. https://doi.org/10.1021/ja407883b.

(39) Deshmukh, P.; Gopinadhan, M.; Choo, Y.; Ahn, S. K.; Majewski, P. W.; Yoon, S. Y.; Bakajin, O.; Elimelech, M.; Osuji, C. O.; Kasi, R. M. Molecular Design of Liquid Crystalline Brush-like Block Copolymers for Magnetic Field Directed Self-Assembly: A Platform for Functional Materials. *ACS Macro Lett.* **2014**, *3* (5), 462–466. https://doi.org/10.1021/mz500161k.

(40) Gopinadhan, M.; Deshmukh, P.; Choo, Y.; Majewski, P. W.; Bakajin, O.; Elimelech, M.; Kasi, R. M.; Osuji, C. O. Thermally Switchable Aligned Nanopores by Magnetic-Field Directed Self-Assembly of Block Copolymers. *Adv. Mater.* **2014**, *26* (30), 5148–5154. https://doi.org/10.1002/adma.201401569.

Chapter 3 – Design, Synthesis and Characterization of a liquid crystalline brush like imidazolium copolymer membranes

3.1 Research objective

The goal of this dissertation is to develop a new platform for the synthesis of a liquid crystalline brush like imidazolium functionalized anion exchange membrane to address the current issues associated with anion exchange membranes such as low hydroxide ion conductivity and lack of mechanical and chemical stability.[1,2]

3.2 An overview of the proposed novel platform for the synthesis of an AEM

The prerequisites for an optimum AEM includes high hydroxide conductivity, chemical and thermal stability at high alkaline environments and sufficient mechanical integrity and resilience for device fabrication and operation.[3] But optimization of all features together could be strenuous as the enhancement of one property could cost the optimum functioning conditions of another property. For instance increase in the ion-conducting groups could lead to membrane swelling and degradation which finally affects the stability of the membrane.[4,5] Previous research studies on AEMs have highlighted that microstructure and phase separation of a polymer has a high impact on both the conductivity and the stability of the membrane.[6] Therefore, the microstructured, self-assembled liquid crystalline block copolymer is a versatile approach to design AEMs with industrially desired properties.

Lately, our group has come up with a novel liquid crystalline brush block copolymer design NBCB-b-NBPLA containing functionalized norbornene polymers. These block copolymers were synthesized via ring-opening metathesis polymerization (ROMP) of norbornene and the major block contains cynobiphenyl mesogens joined by 6 or 12 spacer groups to the norbornene backbone and the minor block contains poly(D, L-lactide) (PLA) chains of various lengths in correlation to Mn of 1, 2 and 3 kg/mol.[7] A self-assembled block copolymer architecture was obtained by the cynobiphenyl units which facilitate the formation of smectic mesophases by magnetic alignment. The minority block is composed of poly(D, L-lactide) (PLA) side chains and it is selectively etched by hydrolysis under gentle alkaline conditions.[8] (Figure 3.1)The selective removal of PLA blocks results in a functionalized nanoporous surface. The use of the polynorbornene backbone permits the system to be crosslinked after magnetic alignment and by this method, mechanically robust membranes could be obtained.

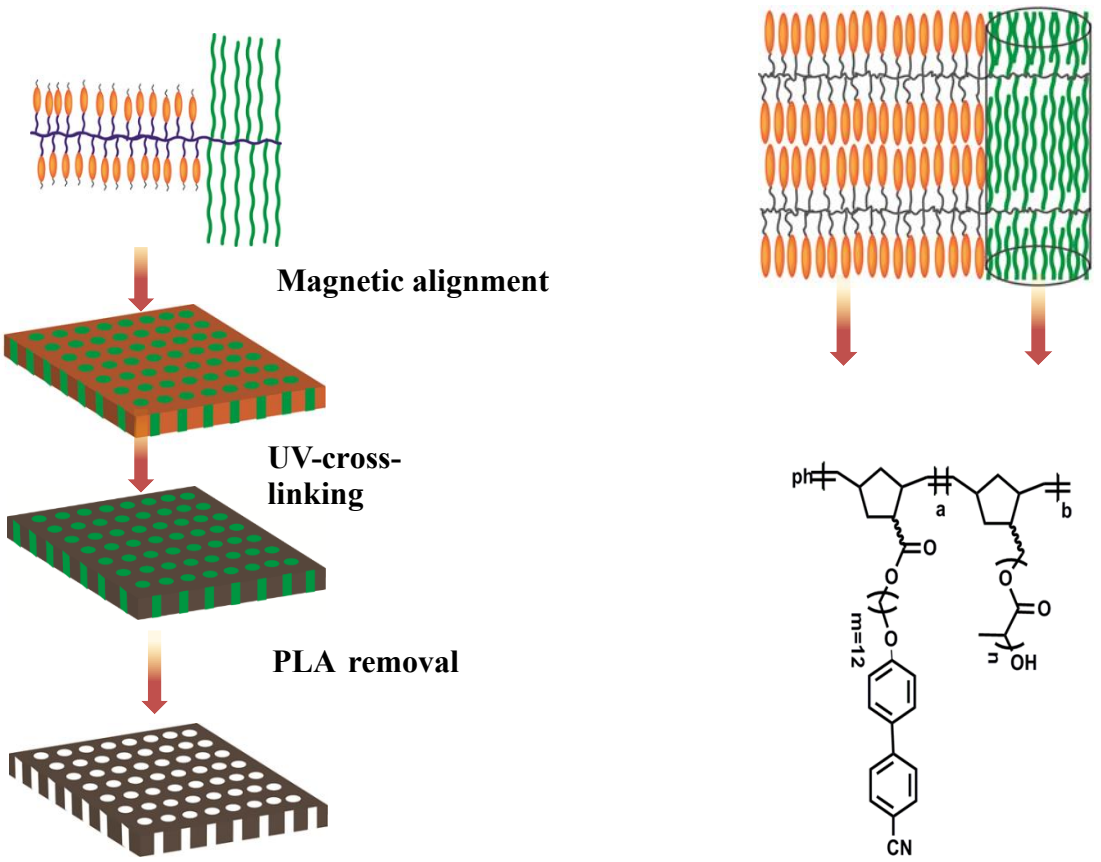

Figure 3. 1: Schematic illustration of a magnetically aligned nanoporous membrane containing NBCB-b-NBPLA obtained by selective removal of PLA. Adapted from reference (8)

Alignment of the domains induces microphase segregation and hence improves ion conductivity. It has been reported that the aforementioned block copolymer architecture will form microdomains 12-15 nm in size which is in the size range of domain sizes of Nafion.[8,9] However one could argue that the alignment of pores could reduce the selectivity towards anions due to the formation of continuous pores. But if the pores are functionalized the selectivity still remains regardless of its alignment and continuity. For instance, if the pores are functionalized with an anion exchanging head group only anions will pass through the pores.

Considering this principle a new platform for the synthesis of an AEM is introduced by fabricating a triblock copolymer containing NBCB, NBPLA and an imidazole functionalized ion-conducting moiety as the third block. (Figure 3.2) The conductivity is expected to be enhanced controlling structure-property relationship of the proposed novel polymer design.

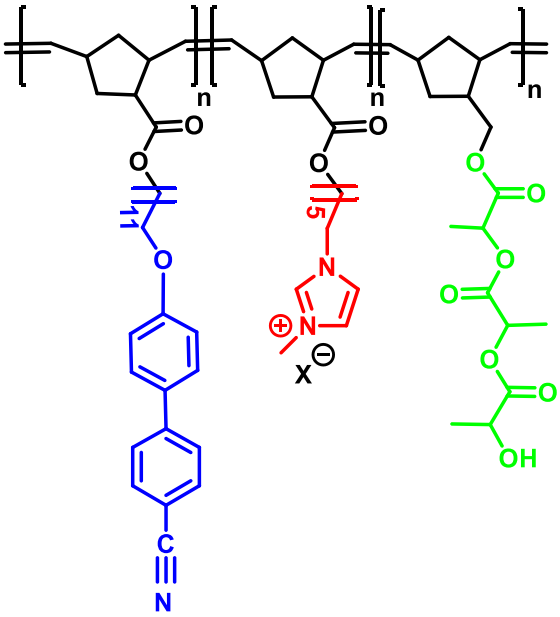

Figure 3. 2: Chemical structure of the proposed triblock copolymer

Norbornene backbone is chosen specifically due to its easy polymerization ability via ROMP, low molar mass, excellent film-forming properties and ability to functionalize and crosslink accordingly.[10,3] The cynobiphenyl functionalized norbornene block is selected as the majority block (70%) to incorporate LC properties to the system and PLA containing norbornene block is selected to obtain a nanoporous structure facilitating the formation of ion channels. The ion-conducting imidazolium functionalized block is chosen as the minority block to get an idea about the lowest ion exchanging capacity of the membrane. Imidazole is chosen over the traditionally used quaternary ammoniums due to it's low susceptibility to hydroxide attack, adaptable chemical structure and selective solubilities leading to a variety of applications.[11,12,13]

3.3 Experimental section

3.3.1 Chemicals

5-Norbornene-2-carboxylic acid (mixture of endo and exo, 98%), 5-norbornene-2-methanol (mixture of endo and exo, 98%), tin(II)-2-ethylhexanoate (95%), 4-dimethylaminopyridine (DMAP, 99%), N,N′-dicyclohexylcarbodiimide (DCC, 99%), N-(3-Dimethylaminopropyl)-N′-ethylcarbodiimide hydrochloride (EDC,98%), Lithium bis(trifluoromethanesulphonyl)imide (LiTFSI) and Grubbs catalyst second generation are purchased from Aldrich and used without further purification. Modified Grubbs catalyst second generation $(H_2IMes)(pyr)_2(Cl)_2RuCHPh$ (mG_2) is synthesized as described in literature.[14] Dry methylene chloride (CH_2Cl_2, 99.8%), anhydrous tetrahydrofuran (THF, 99.9%), anhydrous dimethylformamide (DMF), anhydrous acetonitrile, oxalyl chloride (98%), ethyl vinyl ether (EVE, 99%), 3,6-dimethyl-1,4-dioxane-2,5-dione (D,L-lactide, 99%) are obtained from Acros Organics. 4- S2 Cyano-4'-hydroxyphenyl (98%), 6-bromo1-hexanol (98%), 12-Bromo-1-dodecanol (98%) and 1-Methylimidazole are obtained from TCI America.

3.3.2 Synthesis of monomers

A. Synthesis of mono-substituted cyanobiphenyl norbornene (NBCB12)

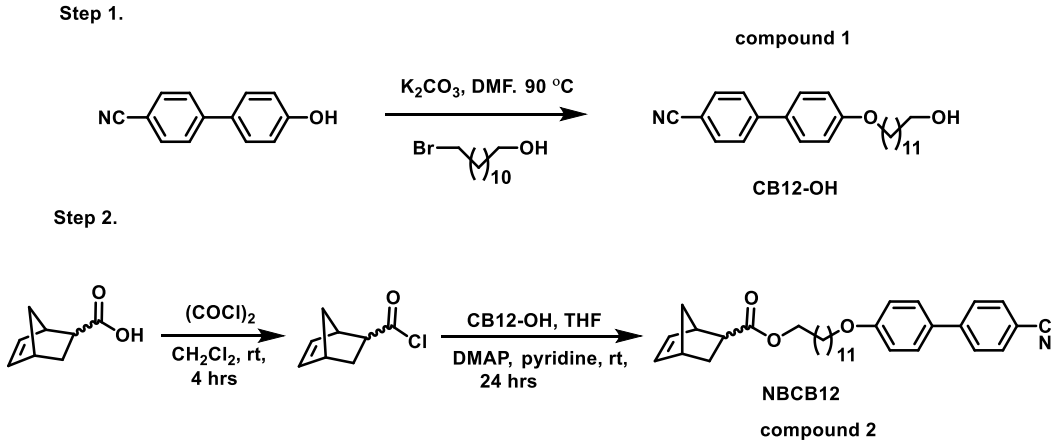

Scheme 3. 1: Synthetic routes for compound 1 and compound 2 (adapted from reference 8)

Compound 1 (CB_{12})

In a round bottom flask equipped with a magnetic stir bar, 12-Bromo-1-dodecanol (14.3 g, 53.8 mmol), 4-cyano-4'-hydroxyphenyl (6.9 g, 35.9 mmol), K_2CO_3 (9.89 g, 72.0 mmol) and DMF (50 mL) are added and sealed with a rubber septum. The reaction mixture is purged with nitrogen for 10 min and then stirred in an oil bath for 48 h at 95 °C. The reaction mixture is cooled down to room temperature and diluted with 70 mL of CH_2Cl_2. The mixture is washed with 200 mL of deionized water twice and treated with 5% NaOH (aq, 100 mL) to remove DMF. The organic layer is separated from the aqueous layer, collected and dried with $MgSO_4$. (Scheme 3.1) The crude product is purified by recrystallization using 50 mL of ethanol. 9.1 g, yield = 67%, ^{1}H NMR (500 S4 MHz, $CDCl_3$): δ 7.5-7.66 (m, 6H, aromatic CH2-), 6.96 (m, 2H, aromatic CH2-), 3.99 (m, 2H, O-CH2-), 3.62 (m, 2H, -CH2-OH), 1.79 (m, 2H, -OCH2-CH2-), 1.27-1.55 (m, 21H, -CH2-).

Compound 2 ($NBCB_{12}$)

Flame dried air-free single neck flask equipped with a bubbler and a magnetic stir bar is charged with 5-norbornene-2-carboxylic acid (86/14 = endo/exo) (4.0 g, 0.028 mol) and 20 mL of CH_2Cl_2, and purged with nitrogen for 10 min. To this solution, excess oxalyl chloride (10 mL, 0.067mol) is injected in a dropwise manner, followed by adding a drop of DMF. After 4 h reaction at room temperature, unreacted oxalyl chloride is removed under reduced pressure, resulting in a pale yellow liquid of norbornene carbonyl chloride, which is further diluted with 20 mL of CH_2Cl_2. To this solution, compound 1 (5.32 g, 0.013 mol) in dry CH_2Cl_2 (30 mL) is added, followed by a catalytic amount of DMAP and pyridine mixture. The reaction mixture is stirred for 12 h at room temperature under nitrogen. Afterward, the reaction mixture is filtered to remove organic salt, and then filtered solution is concentrated using rotary evaporator and precipitated into ethanol. The crude product is purified by column chromatography with ethyl acetate/hexane = 3/7 (v/v) as the mobile phase and silica gel as the stationary phase. The recovered product is further purified by recrystallization using ethanol. Yellow crystalline solid, 3.46 g, yield = 53.3%, ^{1}H NMR (500

MHz, CDCl3, δ): 7.5-7.66 (m, 6H, aromatic CH2-), 6.98 (m, 2H, aromatic CH2-), 5.9-6.2 (m, 2H, cyclic, -CH=CH-, endo/exo), 3.98 (m, 4H, -OCH2-), 2.88-3.18 (m, 3H, cyclic, -CH-, endo/exo), 1.26-1.88 (m, 25H, -CH-).

B. Synthesis of norbornenyl end-functionalized poly(D,L-lactide) (NBPLAy)

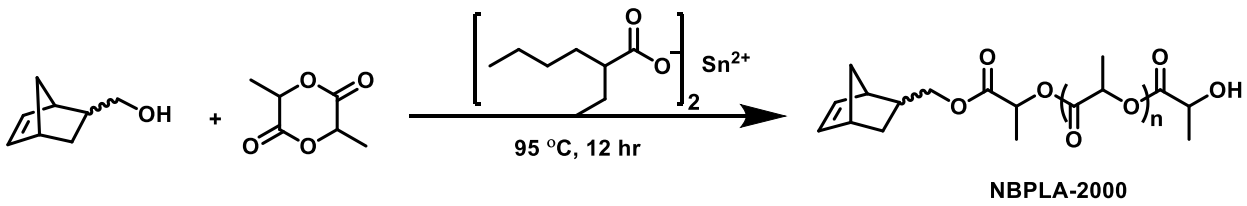

Scheme 3. 2 : Synthetic route for the synthesis of NBPLA (adapted from reference 8)

A flame dried schlenk tube is charged with 5-norbornene-2-methanol (endo/exo = 63/37) (984 mg, 7.93 mmol), D,L-lactide (8.0 g, 55.51 mmol), tin (II) 2-ethylhexanoate (64 mg, 0.016 mmol) and a magnetic stir bar. Using a laboratory schlenk line, the reaction tube is evacuated and backfilled with nitrogen three times. Then, the reaction tube is placed in an oil bath and stirred for 12 h at 100 °C. Afterward, the reaction mixture is cooled to room temperature, diluted with THF, precipitated into methanol, and dried in a vacuum oven for overnight at room temperature. 3.7 g, yield = 41.0%, 1H NMR (500 MHz, CDCl3): δ 5.9-6.2 (m, 2H, -CH=CH-), 5.14 (m, 26H, -CO-CH-), 4.3 (m, 1H, –CH-O-, terminal end), 3.7-4.2 (m, 2H, –OCH2-), 2.7-2.9 (m, 2H, cyclic, -CH- endo/exo), 2.3 (m, 1H cyclic,-CH- endo), 1.3-1.9 (m, 33H, cyclic –CH- and lactide –CH3), 0.51-1.12 (m, 1H, cyclic,-CH- endo/exo), Mn (1H NMR) = 1990 g/mol, Mn (GPC-ELSD) = 2,600 g/mol, PDI = 1.07.

C. Synthesis of 5-norbornene-2-carboxylate-6- bromohexane (NB(CH_2)$_6$Br), 5-norbornene-2-carboxylate-1-hexyl-3-methyl-imidazolium bromide (NB IM Br) and 5-norbornene-2-carboxylate-1-hexyl-3-methyl-imidazolium bis((trifluoromethyl)sulfonyl)amide (NB IM TFSI)

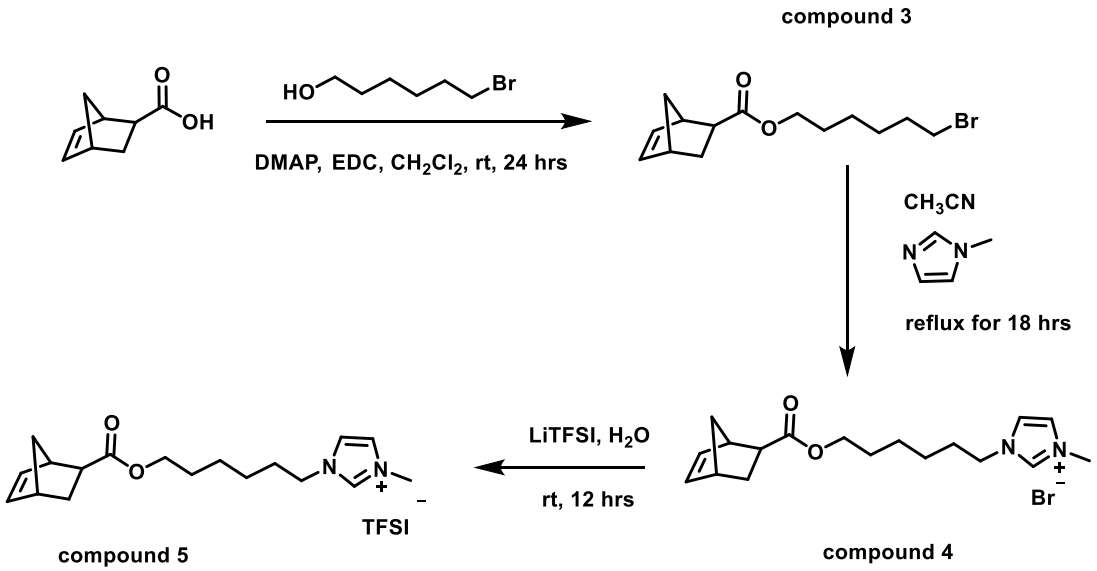

Scheme 3. 3: Synthetic routes for compound 3 (5-norbornene-2-carboxylate-6- bromohexane) compound 4 (5-norbornene-2-carboxylate-1-hexyl-3-methyl-imidazole) and compound 5 ((5-norbornene-2-carboxylate-1-hexyl-3-methyl-imidazolium bis((trifluoromethyl)sulfonyl)amide (Adapted from [13])

In a dried round-bottomed flask equipped with a magnetic stir bar, 5-norbornene-2- carboxylic acid (3.6 g, 0.026 mol) and 6-bromo-1-hexanol (4 g, 0.022 mol) are dissolved with the help of 30 mL of CH_2Cl_2. Then EDC (6.35 g, 0.033 mol) and a catalytic amount of DMAP and pyridine mixture are added to the reaction mixture stirring at room temperature for 12 h, then the reaction is quenched by adding water (30 mL). The crude product is extracted three times with CH_2Cl_2 and the organic layer is dried with anhydrous MgSO4. Then the organic layer is filtered, and concentrated by rotary evaporator to afford an oil product. The crude product is further purifed by column chromatography using hexanes/EtOAc (20 : 1) as the mobile phase and silica gel as the stationary phase to yield a yellow viscous oil (5.04 g, 76%)(compound 3). ^{1}H NMR (500 MHz, $CDCl_3$): δ 6.17–5.85 (m, 2H), 4.01 (t, 2H), 3.36 (t, 2H), 3.17 (s, 1H), 2.99 - 2.85 (m, 2H), 2.13–2.22 (m, 3H), 1.92–1.79 (m, 2H), 1.68–1.21 (m, 7H).

D. Synthesis of 5-norbornene-2-carboxylate-1-hexyl-3-methyl-imidazolium (compound 4 and 5)

Compound 3 (5.0 g, 0.016 mol) and 1-Methylimidazole (1.75 mL, 0.024 mol) are refluxed in acetonitrile for 18 h. After cooling to room temperature, the reaction mixture is concentrated by rotary evaporator to afford yellow viscous oil and then washed with Et2O (3 × 100 mL) to obtain compound 4 (NB IM Br^-)(4.46 g, 80% yield). The resulting oil is dissolved in H_2O (100 mL), LiTFSI (4.88 g, 0.017 mol) is added, and the mixture is stirred at room temperature for 12 h. The yellow oil is extracted with dichloromethane and the organic layer is washed with water and dried over anhydrous MgSO4. Compound 5 (NB IM TFSI) is obtained as yellow oil (4.63 g, 75%). 1H NMR (500 MHz, CDCl3): δ=8.69(s, 1H), 7.30(d, 2H), 6.13-5.86(m, 2H), 4.11(t, 2H), 3.96(t, 2H), 3.71(s, 3H), 3.15 (s, 1H), 1.84 (m, 2H), 1.82 (m, 3H), 1.58-1.55(m, 2H), 1.35-1.24 (m, 7H).

3.3.3 Polymer Synthesis

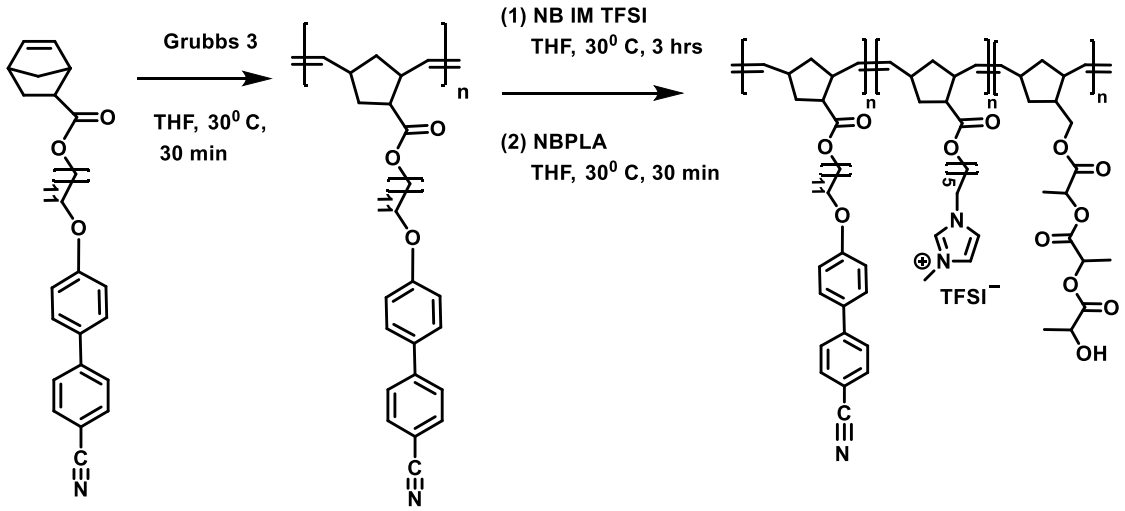

Scheme 3. 4: Synthetic route for new AEM platform

A. Synthesis of Triblock copolymer $NBCB_{12}$: NB IM X: NBPLA 2K

A ring-opening metathesis polymerization (ROMP) of functionalized norbornene monomers is carried out. $NBCB_{12}$ (300 mg, 0.6 mmol) dissolved in 10 mL of CH_2Cl_2 is added to a clean round-bottomed flask equipped with a magnetic stir bar and a rubber septum and purged with nitrogen for 10 min. In a scintillation vial, Grubbs 3 modified (12.5 mg, 0.018 mmol) is dissolved in CH_2Cl_2 (5 mL) and purged with nitrogen for 10 min. Then, it is added to the round bottom flask containing $NBCB_{12}$ and the reaction is allowed for 30 min at room temperature. After the first polymerization is complete, pre-purged CH_2Cl_2 solution containing NB IM X (24 mg, 0.05 mmol) is added and stirred for another 3 hours. Once the second polymerization is complete, pre purged CH_2Cl_2 solution containing NBPLA 2K (106 mg, 0.05 mmol) is added and stirred for another 30 minutes. Then, the reaction is terminated by adding excess EVE. The resulting polymer is precipitated into

a methanol-isopropanol mixture, filtered, and dried in a vacuum oven for overnight at room temperature.

3.3.4 Preparation of nanoporous thin films

A. Representative procedure for crosslinking procedure

200 mg of the triblock copolymer ($NBCB_{12}$: NB IM X: NBPLA 2K), 5 mg of 2-Hydroxy-4′-(2-hydroxyethoxy)-2- methylpropiophenone, and 12 mg of 1,10-decanedithiol are weighed in separate vials covered in aluminum foil. 1 mL of THF is added to the vials to dissolve the contents and are mixed thoroughly. The solvent is then evaporated completely by purging Nitrogen for a few minutes and vacuum drying overnight. Then a thin film was obtained by compression molding at 82°C and quenched to room temperature. This is followed by UV-crosslinking for 3 hours resulting in a crosslinked film. The crosslinking density 36% as determined by gel fraction in THF.

B. Etching of crosslinked films to remove PLA

The crosslinked film sample prepared as described in 3.3.4 A, is immersed in a solution of 0.5M NaOH prepared in 6:4 (water : methanol) mixture and kept at 50 ºC for 5 days. After that, the nanoporous membrane thus formed is washed thoroughly with distilled water to remove any residue left after etching. It is then vacuum dried overnight and characterized using FTIR.[15,16]

3.3.5 Determination of Ion exchange capacity(IEC)

The thin films obtained are pretreated as follows to activate the membrane before taking IEC measurements.[17,18] The activation procedure consists of the alternating conversion of the membrane to OH^- and H^+. The dry weight of the membranes of 1 cm * 1 cm specimens are recorded and then immersed in distilled water for 24 hours. Then the membranes are exposed to a solution of 0.1 M NaOH solution for 2 hours. After washing them thoroughly with distilled water the membranes are then immersed in a solution of 0.1 M HCl for overnight. Thoroughly washed membranes are again immersed in a solution of 0.1 M NaOH for 4 hours and finally immersed in distilled water for 24 hours.

A. Potentiometric method for IEC determination

The pretreated membrane samples are changed into the OH^- form by exposing it in a solution of 1M NaOH for 12 hours. Then they are washed immensely using distilled water to remove excess OH^- ions and immersed in a solution of 0.1 M NaCl solution bubbled with Argon. Due to the excess of chlorides ions OH^- ions attached to the charged groups of the membrane are replaced with chloride ions. The change in the solution pH is measured using a glass pH electrode and the exchanged moles of OH^- is determined using a calibration curve. The calibration curve is acquired by first stabilizing the glass pH electrode in a 0.1M NaCl solution. Once the electrode signal has stabilized 0.05 mL aliquots of 0.01 M NaOH is added by recording the pH after each dose.

B. Spectrophotometric method for IEC determination

This method depends on the number of moles of NO_3^- exchanged for Cl^- ions attached to the membrane. The sample is immersed in a solution of 1 M KNO_3 for a day and then after washing thoroughly with distilled water to remove excess nitrate ions, it is immersed in a solution of a known volume of 0.1 M NaCl. Finally, the concentration of NO_3^- in the solution of 0.1 M NaCl is measured using a UV-Vis spectrophotometer at 210 nm.

3.4 Measurements

^{1}H NMR spectroscopy is conducted on Bruker DMX 500 MHz NMR spectrometer with $CDCl_3$ as solvent at room temperature. ^{1}H NMR chemical shifts are delineated in ppm downfield from TMS. The molecular weight of NBPLA is determined by Gel permeation chromatography (GPC) using a Waters 1515 coupled with a PL-ELS1000 evaporative light scattering (ELS) detector and a Waters 2487 dual-wavelength absorbance UV-Vis detector with tetrahydrofuran (THF) as eluent and polystyrene (PS) standards for constructing a conventional calibration curve. Differential scanning calorimetry (DSC) is conducted on TA-2920 instrument (Q-200 series) calibrated with an Indium standard. The amount of sample used is 5-10 mg and the scanning rate is 10 °C/min. Phase transition temperatures are determined by the first cooling cycle using Universal Analysis software. Thermogravimetric analysis is performed using 5-10 mg of the sample on a TGA Q500 1732 for analysis of thermal properties at 20˚ C/min under Nitrogen. Attenuated infrared (ATIR) spectra are recorded on a diamond ATIR spectrometer. Scanning electron microscope (SEM) images of all samples are recorded using an FEI Teneo LVSEM equipped with an ETD detector with an accelerating voltage 15 kV. The film samples are prepared by compression molding and sputter coated with a thin gold conductive layer before imaging. The IEC measurements are performed using a precise glass pH electrode and spectroscopic data is obtained from Perkin Elmer lambda 1050 UV/VIS/NIR spectrometer.

3.5 Results and Discussion

3.5.1 Charachterization of the monomers and the polymers

The chemical structures of the monomers and triblock copolymers are conformed by ^{1}H NMR as shown below.

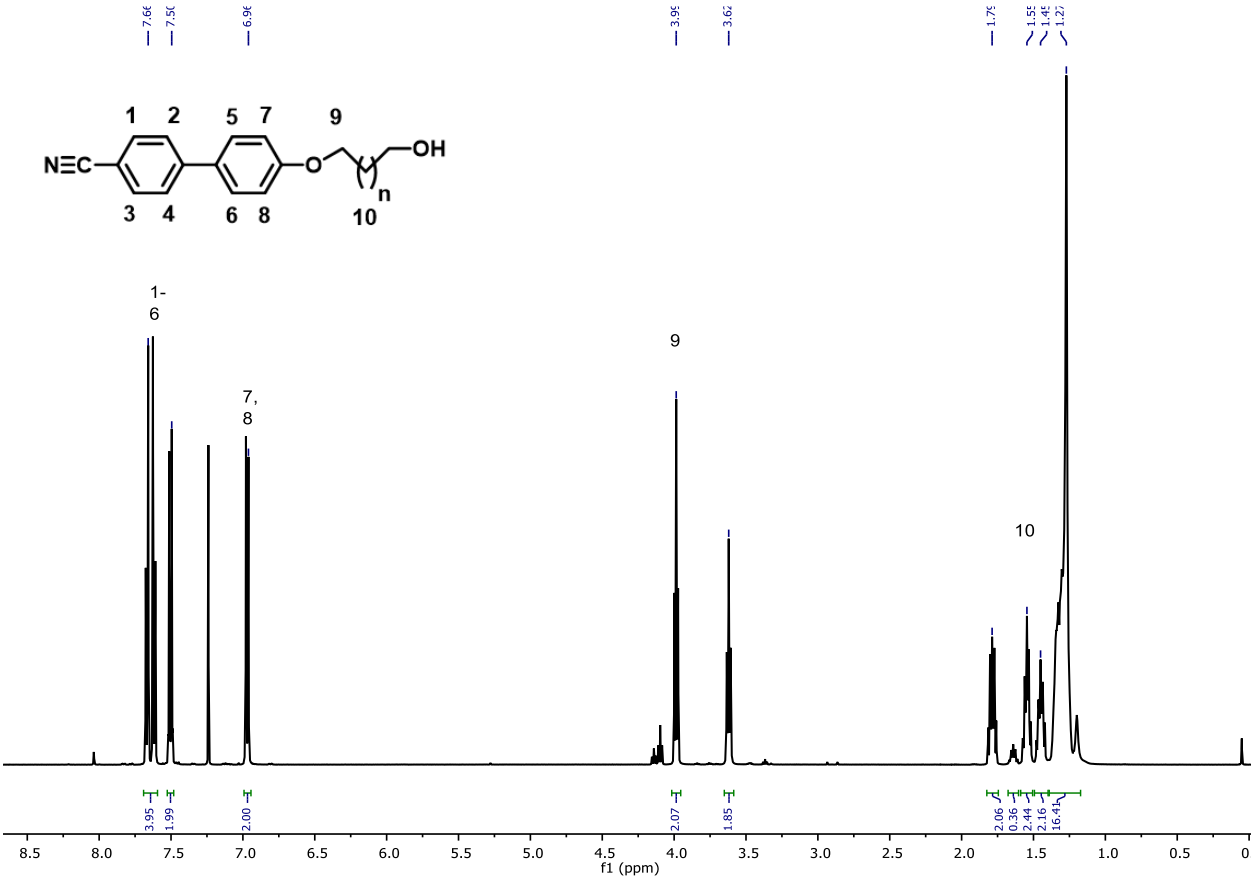

Figure 3. 3: ^{1}H NMR of CB_{12}

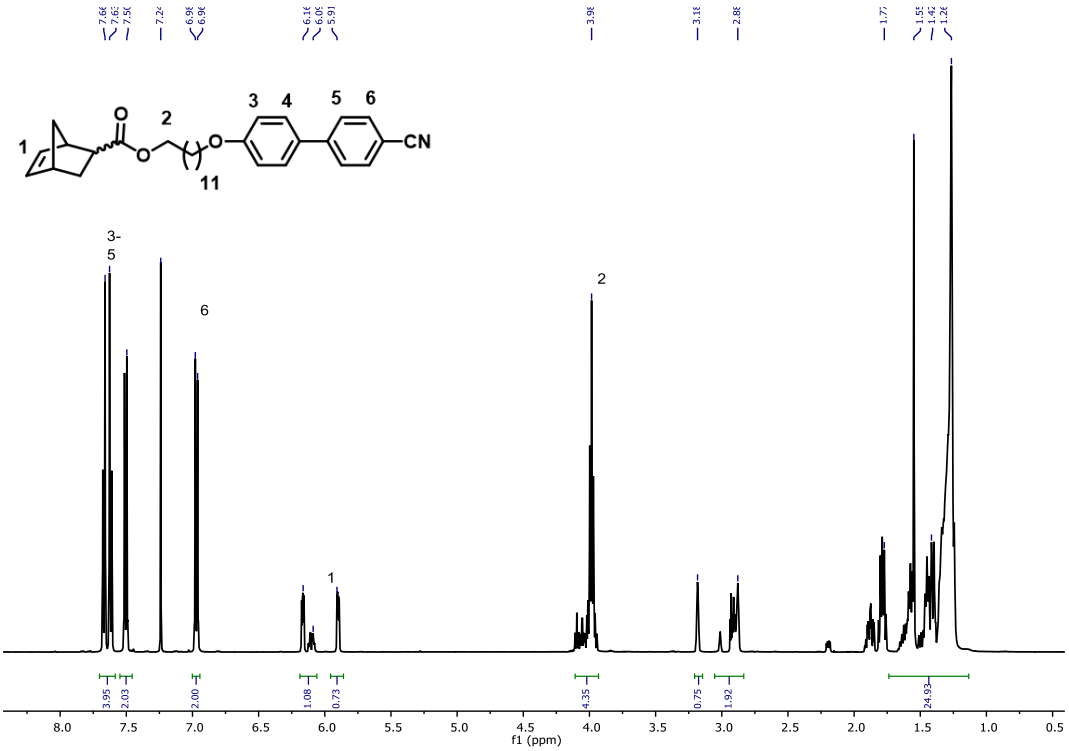

Figure 3. 4: ^{1}H NMR of $NBCB_{12}$

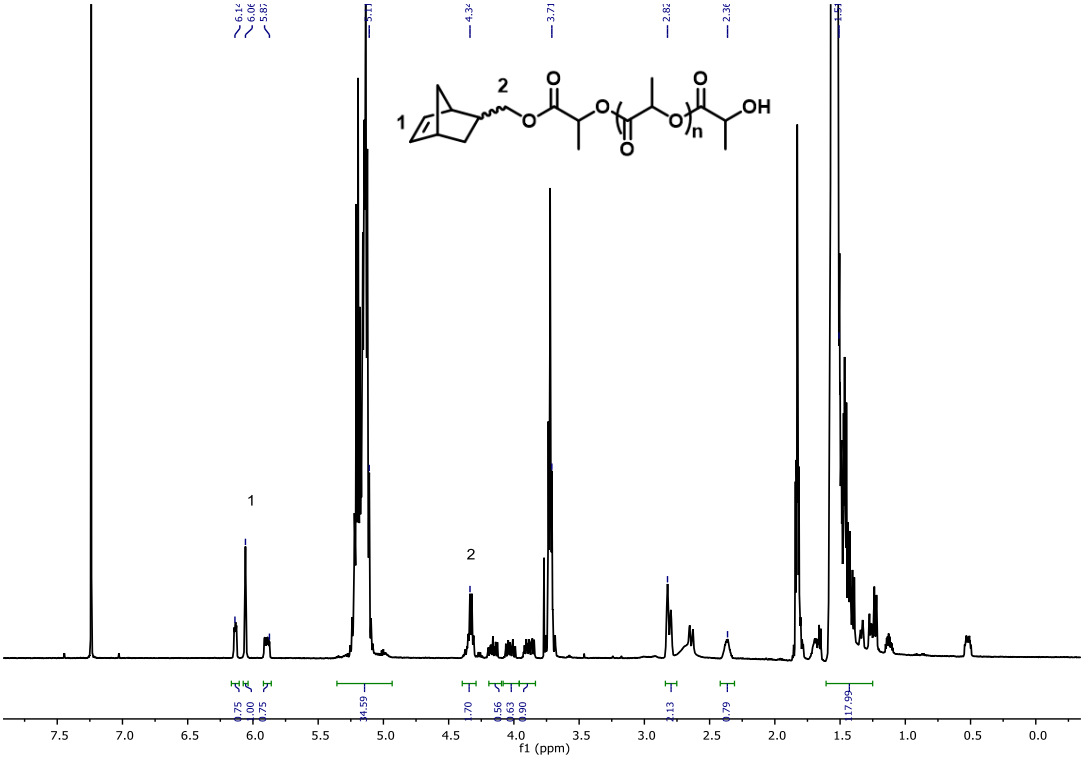

Figure 3. 5: ^{1} HNMR of NBPLA 2K

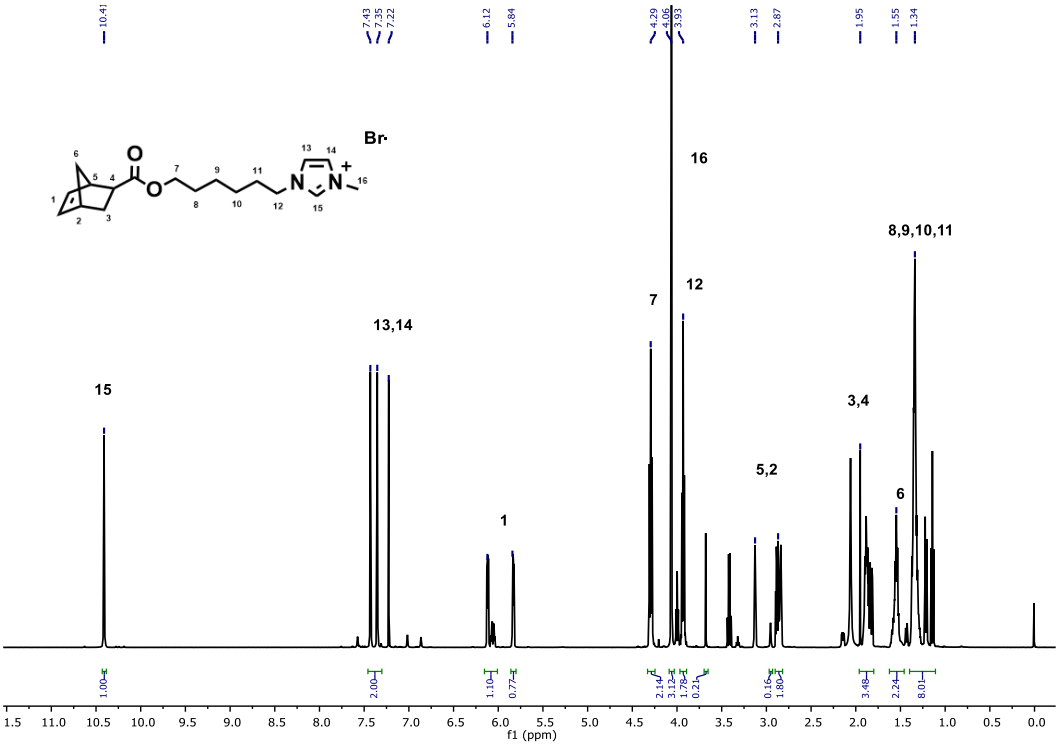

Figure 3. 6: [1]HNMR of NB IM Br

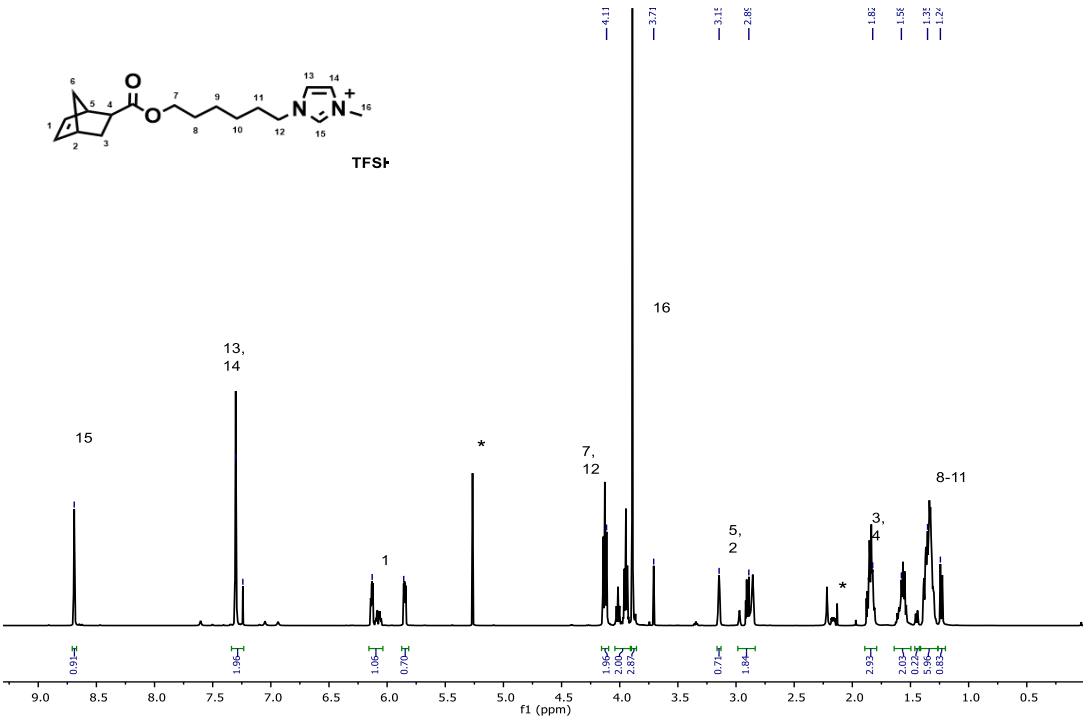

Figure 3. 7: 1H NMR of NB IM TFSI

The characteristic proton absorption peak for the double bond of norbornene monomers appear at 6.12-5.88 ppm (Figure 3.4 – Figure 3.7) and when they polymerize the peak shifts to 5.50-5.10 ppm. The characteristic proton absorption peaks for imidazolium ring appear at 10.41 ppm in NB IM Br and 8.7 ppm in NB IM TFSI.When they polymerize the peak broadens but remains at the same position. The successful synthesis of the monomers and triblock copolymers were confirmed by the 1H NMR spectra.

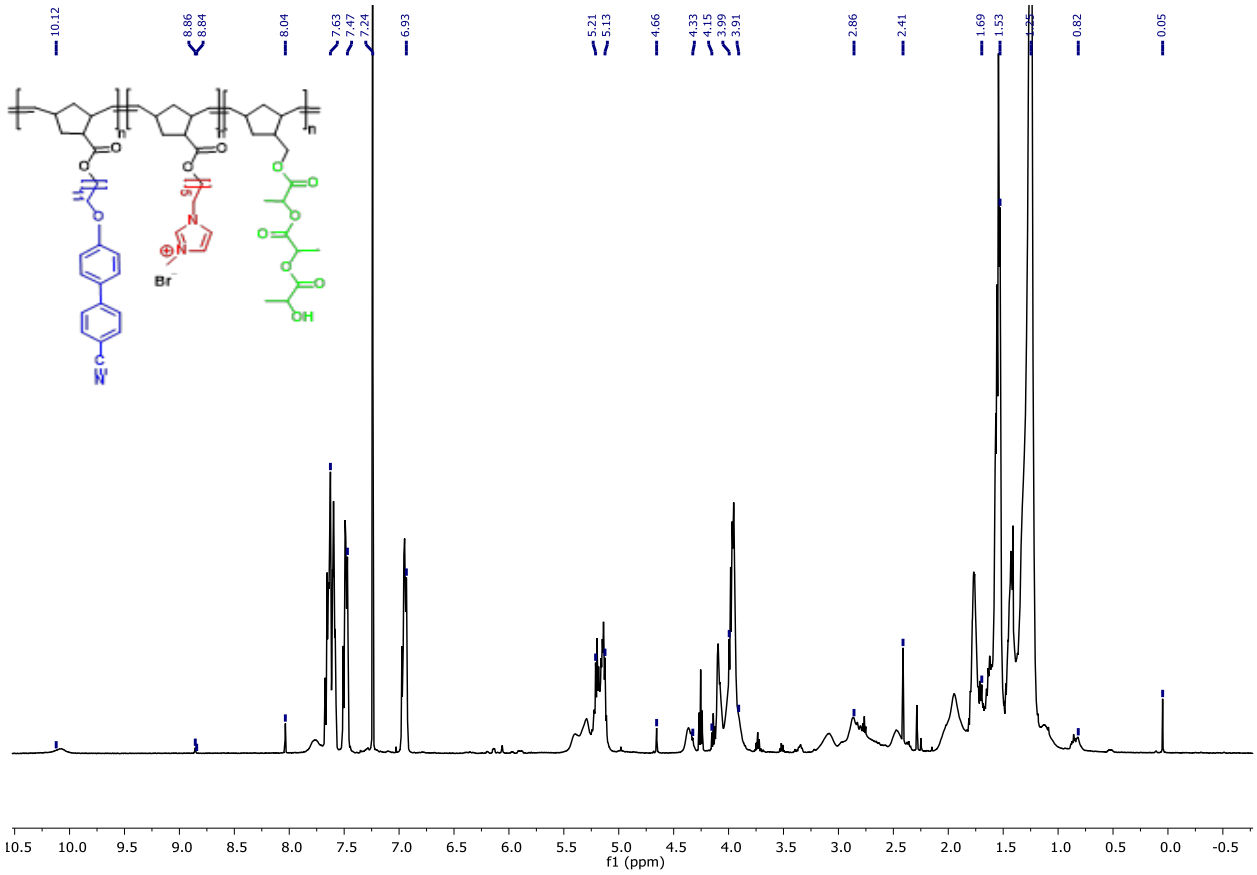

Figure 3. 8: ^{1}H NMR of the triblock copolymer $NBCB_{12}$: NB IM Br: NBPLA 70: 5: 25 by composition

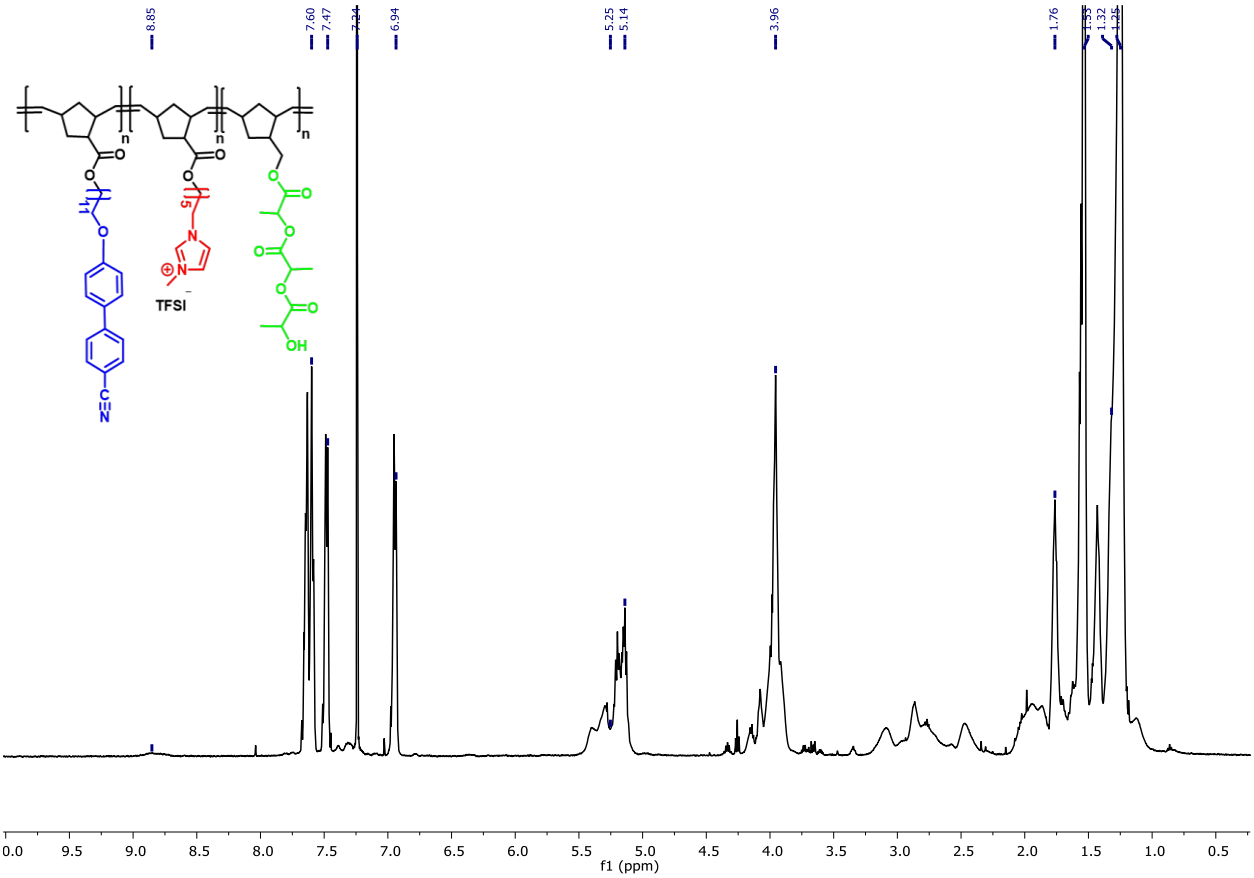

Figure 3. 9: ^{1}H NMR of the triblock copolymer $NBCB_{12}$: NB IM TFSI: NBPLA 70: 5: 25 by the composition

3.5.2 Thermal properties

Thermal properties of the triblock copolymers were analyzed by differential scanning calorimetry (DSC) and thermogravimetry analysis (TGA). According to TGA curves, both triblock copolymers exhibit excellent thermal stability with 5% weight loss, triblock containing NB IM Br at 267.42˚C (Figure 3.10) and triblock containing NB IM TFSI at 300.65˚ C (Figure 3.11). Also, an idea of how thermal properties behave with crosslinking and etching was also obtained by TGA curves where crosslinked polymers exhibit much higher thermal stability compared to the others. (Figure 3.12).

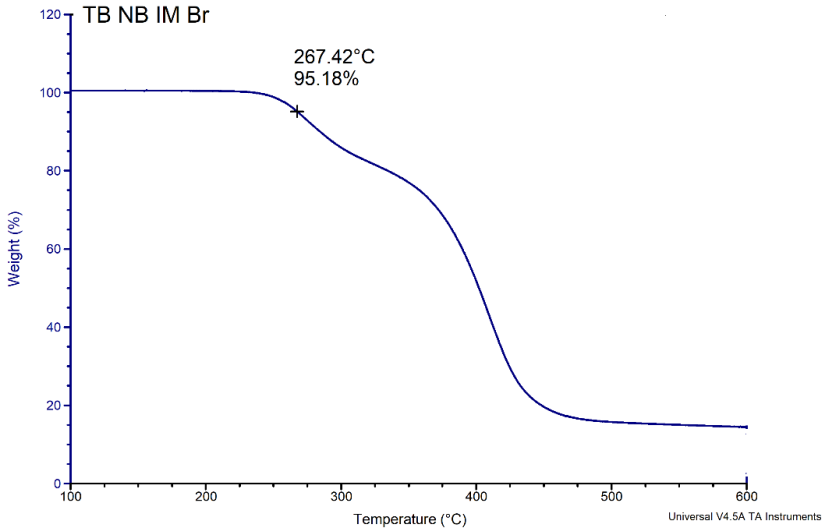

Figure 3. 10: The TGA curve of the triblock containing NB IM Br

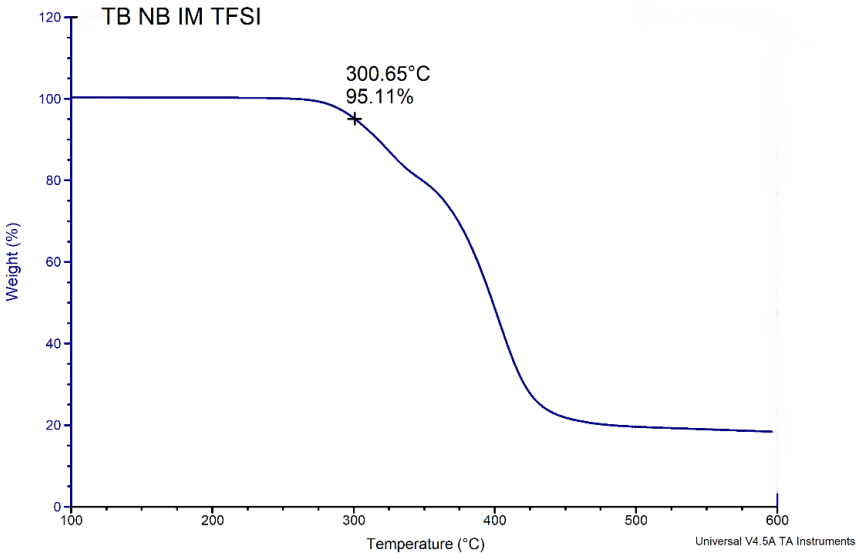

Figure 3. 11: The TGA curve of the triblock containing NB IM TFSI

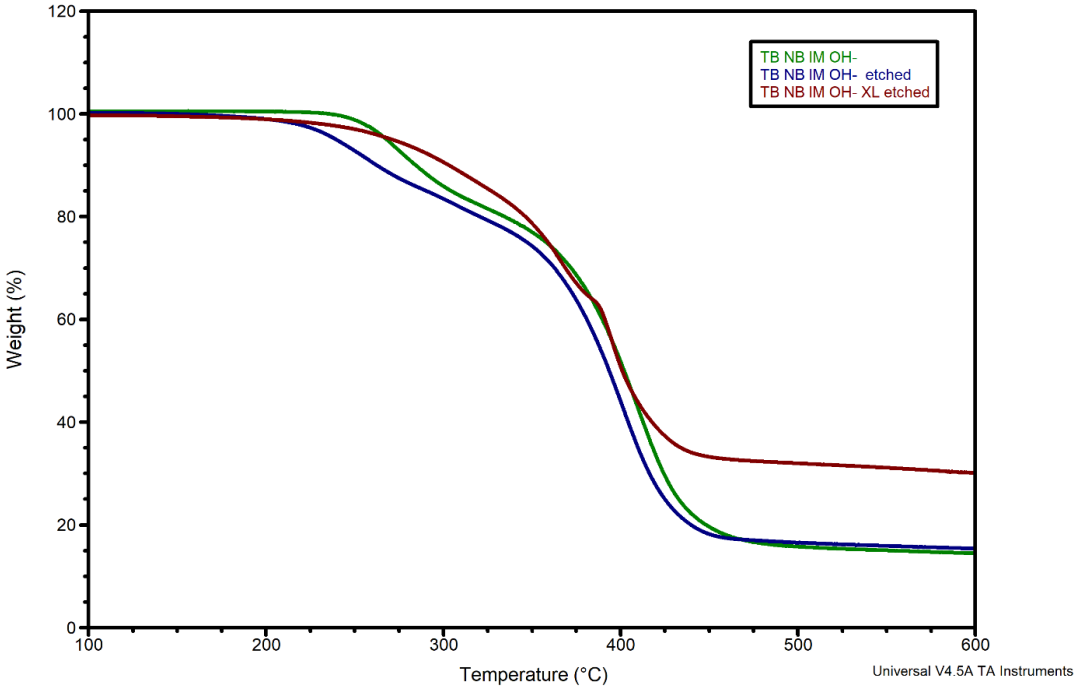

Figure 3. 12: Thermal property of the polymers after crosslinking and etching(XL- crosslinked, etched- PLA domains removed under mild basic conditions)

The differential scanning calorimetry curves were obtained to see the phase transitions of the polymer and both the triblock copolymers exhibit glass transition temperature around 17-18˚ C and liquid crystalline temperature around 73-75˚ C indicating that the blocks have strong microphase separation. (Figure 3.13). All the samples were heated upto 250˚C to remove thermal history and the first cooling circle was used to interpret the data.

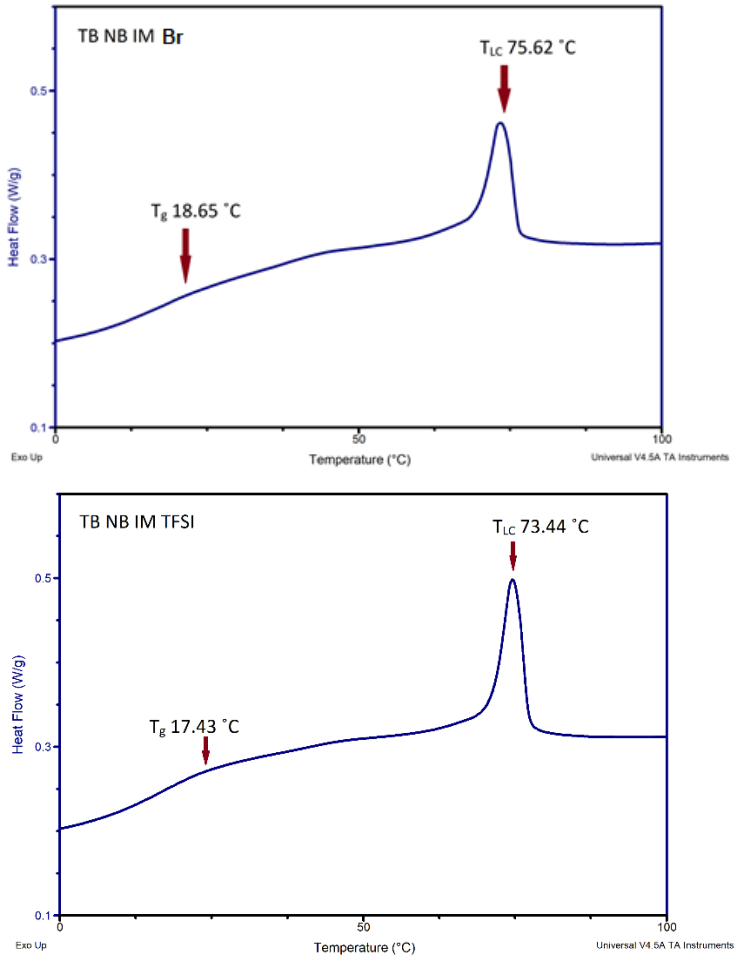

Figure 3. 13: DSC curves of the triblock copolymers

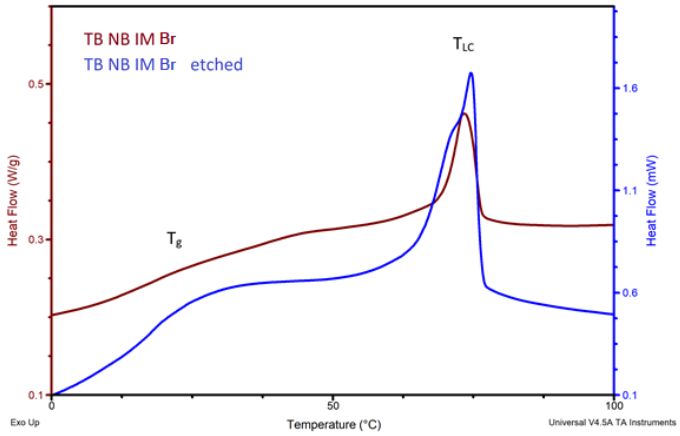

Figure 3. 14: DSC curves of the etched vs non-etched triblock copolymers (etched- PLA domains removed under mild basicconditions)

3.5.3 Morphology of the copolymers

The etching of the membrane to form a nanoporous membrane was checked using ATIR and SEM imaging. The shoulder peak at the wavelength 1752 cm^{-1} of un-etched triblock copolymers disappears after etching indicating the removal of PLA.

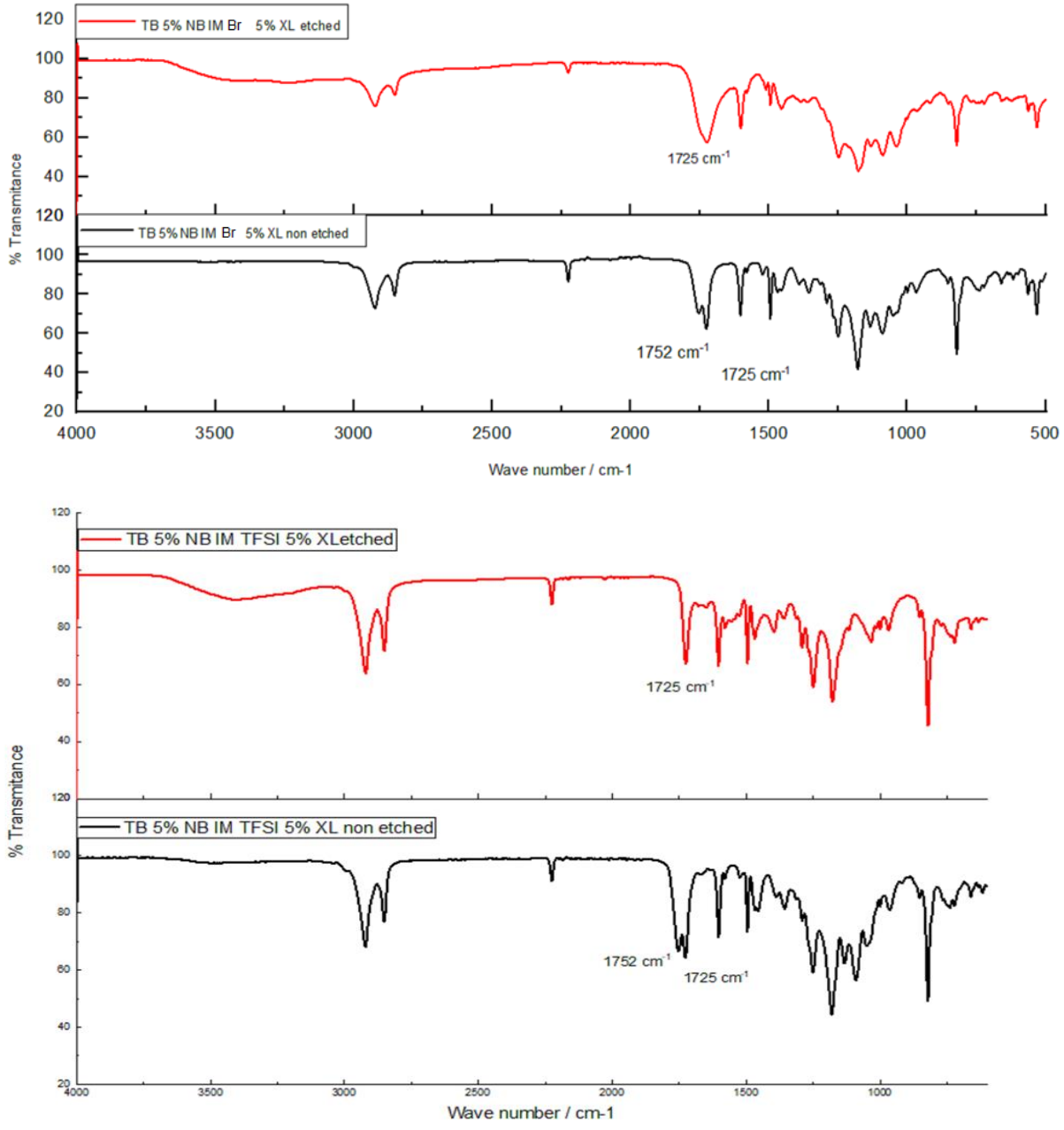

Figure 3. 15: FTIR spectrum of the etched and non-etched copolymers(etched-PLA domains removed under mild basic conditions)

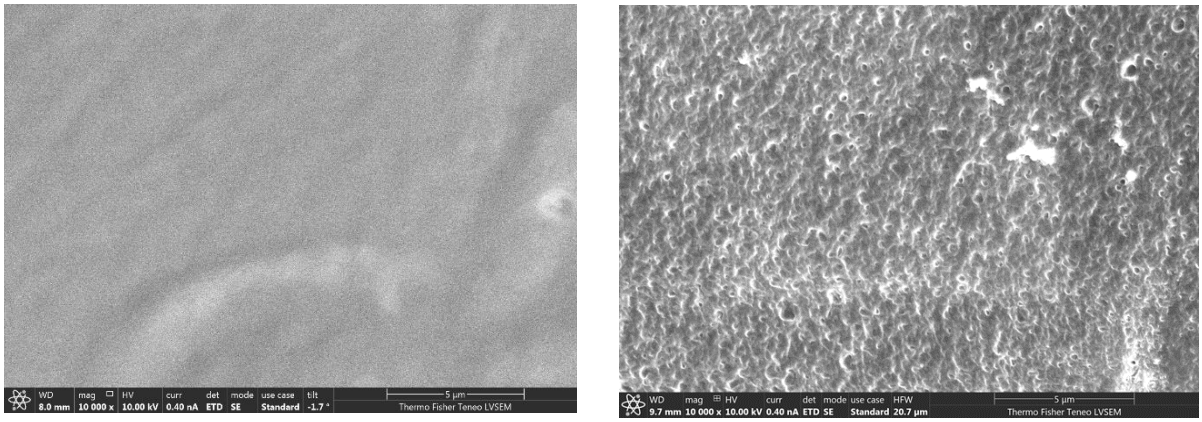

(a) (b)

Figure 3. 16: Comparison of SEM images of gold sputter-coated (a) crosslinked, unetched triblock copolymer NB IM Br 5% by composition thin-film vs (b) etched film with nanopores (etched-PLA domains removed under mild basic conditions)

3.5.4 Ion Exchange capacity

The Ion exchange capacity of the thin films was measured by both potentiometric and spectroscopic methods as described in section 3.3.5 and the IEC value was calculated as follows.

$$IEC = \frac{no.\,of\ moles\ of\ ions\ exchanged\ (mmol)}{dry\ weight\ of\ the\ membrane\ (g)}$$

The IEC values of the films were measured under different crosslinking and etching conditions and are summarized in the table below. All measurements were repeated thrice and the average ion exchange capacity is calculated. Accroding to the data highest IEC was observed in membranes that are both etched and crosslinked in both membranes TB NB IMBr and TB NB IMTFSI which contains only 5% of the ion conducting block by composition. The IEC observed for TB NB IMBr from potentiometry is 0.0115 mmol/g and 0.0084 mmol/g from UV-Vis spectroscopic data. Similarly the IEC values for TB NB IMTFSI are 0.0168 mmol/g from potentiometry and 0.0261mmol/g from UV/Vis data.

Thin film	Etched	Crosslinked	Avg IEC from potentiometry	Avg IEC from spectroscopy
TB NB IM Br 5%	-	-	0.0034	0.0021
TB NB IM Br 5%	✓	-	0.0087	0.0063
TB NB IM Br 5%	-	✓	0.0041	0.0026
TB NB IM Br 5%	✓	✓	0.0115	0.0084
TB NB IM TFSI 5%	-	-	0.0045	0.0034
TB NB IM TFSI 5%	✓	-	0.0062	0.0051
TB NB IM TFSI 5%	-	✓	0.0035	0.0021
TB NB IM TFSI 5%	✓	✓	0.0168	0.0261

Table 1: Summary table of ion exchange capacity in mmol/g of crosslinked (5%) and etched samples where the PLA domains have been removed under mild basic conditions

3.6 Conclusions

In this study, we describe the synthesis of a novel brush like liquid crystalline imidazolium functionalized polymers by ring-opening metathesis polymerization, that can be used as an anion exchange membrane for fuel cells and water electrolysis applications. Here we introduce a new synthetic platform to obtain a polymer architecture with a well-defined microstructure facilitating the ion conductivity through the formation of ion channels. The majority block contains a side-chain LC block which provides a high degree of order due to their ability to align due to an applied external field and the PLA side chain block allows the formation of nanopores. These nanopores can be functionalized by first aligning copolymer into cylindrical PLA domains by compression molding and then selectively etching the PLA.

The triblock copolymers depict good thermal stability and two thermal transitions illustrating the significant microphase separation of the blocks. This makes it a good candidate for the fuel cell and water electrolysis applications which are typically operated around 150˚C. The IEC was determined using potentiometry and UV-Vis Spectroscopy and highest IEC was observed for films which are both crosslinked and etched. This illustrates that the formation of nanopores facilitates ion conduction.

3.7 References

(1) Hagesteijn, K. F. L.; Jiang, S.; Ladewig, B. P. A Review of the Synthesis and Characterization of Anion Exchange Membranes. *Journal of Materials Science*. 2018, pp 11131–11150. https://doi.org/10.1007/s10853-018-2409-y.

(2) Gao, X.; Yu, H.; Jia, J.; Hao, J.; Xie, F.; Chi, J.; Qin, B.; Fu, L.; Song, W.; Shao, Z. High Performance Anion Exchange Ionomer for Anion Exchange Membrane Fuel Cells. *RSC Adv.* **2017**, *7* (31), 19153–19161. https://doi.org/10.1039/c7ra01980g.

(3) Chen, W.; Mandal, M.; Huang, G.; Wu, X.; He, G.; Kohl, P. A. Highly Conducting Anion-Exchange Membranes Based on Cross-Linked Poly(Norbornene): Ring Opening Metathesis Polymerization. *ACS Appl. Energy Mater.* **2019**, *2* (4), 2458–2468. https://doi.org/10.1021/acsaem.8b02052.

(4) Pan, J.; Chen, C.; Li, Y.; Wang, L.; Tan, L.; Li, G.; Tang, X.; Xiao, L.; Lu, J.; Zhuang, L. Constructing Ionic Highway in Alkaline Polymer Electrolytes. *Energy Environ. Sci.* **2014**, *7* (1), 354–360. https://doi.org/10.1039/c3ee43275k.

(5) Hossain, M. M.; Wu, L.; Liang, X.; Yang, Z.; Hou, J.; Xu, T. Anion Exchange Membrane Crosslinked in the Easiest Way Stands out for Fuel Cells. *J. Power Sources* **2018**, *390*, 234–241. https://doi.org/10.1016/j.jpowsour.2018.04.064.

(6) He, Y.; Si, J.; Wu, L.; Chen, S.; Zhu, Y.; Pan, J.; Ge, X.; Yang, Z.; Xu, T. Dual-Cation Comb-Shaped Anion Exchange Membranes: Structure, Morphology and Properties. *J. Memb. Sci.* **2016**, *515*, 189–195. https://doi.org/10.1016/j.memsci.2016.05.058.

(7) Gopinadhan, M.; Deshmukh, P.; Choo, Y.; Majewski, P. W.; Bakajin, O.; Elimelech, M.; Kasi, R. M.; Osuji, C. O. Thermally Switchable Aligned Nanopores by Magnetic-Field Directed Self-Assembly of Block Copolymers. *Adv. Mater.* **2014**, *26* (30), 5148–5154. https://doi.org/10.1002/adma.201401569.

(8) Deshmukh, P.; Gopinadhan, M.; Choo, Y.; Ahn, S. K.; Majewski, P. W.; Yoon, S. Y.; Bakajin, O.; Elimelech, M.; Osuji, C. O.; Kasi, R. M. Molecular Design of Liquid Crystalline Brush-like Block Copolymers for Magnetic Field Directed Self-Assembly: A Platform for Functional Materials. *ACS Macro Lett.* **2014**, *3* (5), 462–466. https://doi.org/10.1021/mz500161k.

(9) Ndaya, D.; Bosire, R.; Mahajan, L.; Huh, S.; Kasi, R. Synthesis of Ordered, Functional, Robust Nanoporous Membranes from Liquid Crystalline Brush-like Triblock Copolymers. *Polym. Chem.* **2018**, *9* (12), 1404–1411. https://doi.org/10.1039/c7py02127e.

(10) Clark, T. J.; Robertson, N. J.; Kostalik IV, H. A.; Lobkovsky, E. B.; Mutolo, P. F.; Abruña, H. D.; Coates, G. W. A Ring-Opening Metathesis Polymerization Route to Alkaline Anion Exchange Membranes: Development of Hydroxide-Conducting Thin Films from an Ammonium-Functionalized Monomer. *J. Am. Chem. Soc.* **2009**, *131* (36), 12888–12889. https://doi.org/10.1021/ja905242r.

(11) Guo, D.; Lai, A. N.; Lin, C. X.; Zhang, Q. G.; Zhu, A. M.; Liu, Q. L. Imidazolium-Functionalized Poly(Arylene Ether Sulfone) Anion-Exchange Membranes Densely Grafted with Flexible Side Chains for Fuel Cells. *ACS Appl. Mater. Interfaces* **2016**, *8* (38), 25279–25288. https://doi.org/10.1021/acsami.6b07711.

(12) Price, S. C.; Williams, K. S.; Beyer, F. L. Relationships between Structure and Alkaline Stability of Imidazolium Cations for Fuel Cell Membrane Applications. *ACS Macro Lett.* **2014**, *3* (2), 160–165. https://doi.org/10.1021/mz4005452.

(13) Wang, J.; He, X.; Zhu, H.; Chen, D. Preparation of a ROMP-Type Imidazolium-Functionalized Norbornene Ionic Liquid Block Copolymer and the Electrochemical Property for Lithium-Ion Batteries Polyelectrolyte Membranes. *RSC Adv.* **2015**, *5* (54), 43581–43588. https://doi.org/10.1039/c5ra04860e.

(14) Xia, Y.; Olsen, B. D.; Kornfield, J. A.; Grubbs, R. H. Efficient Synthesis of Narrowly Dispersed Brush Copolymers and Study of Their Assemblies: The Importance of Side Chain Arrangement. *J. Am. Chem. Soc.* **2009**, *131* (51), 18525–18532. https://doi.org/10.1021/ja908379q.

(15) Zalusky, A. S.; Olayo-Valles, R.; Wolf, J. H.; Hillmyer, M. A. Ordered Nanoporous Polymers from Polystyrene-Polylactide Block Copolymers. *J. Am. Chem. Soc.* **2002**, *124* (43), 12761–12773. https://doi.org/10.1021/ja0278584.

(16) Hegazy, T. M.; Shoeib, M. Y.; Hassan, G. M. Study on the Effect of NaOH Concentration and Etching Duration on Some Properties of γ-Irradiated PADC. *Beni-Suef Univ. J. Basic Appl. Sci.* **2013**, *2* (1), 36–40. https://doi.org/10.1016/j.bjbas.2013.09.005.

(17) Hnát, J.; Paidar, M.; Schauer, J.; Žitka, J.; Bouzek, K. Polymer Anion-Selective Membranes for Electrolytic Splitting of Water. Part II: Enhancement of Ionic Conductivity and Performance under Conditions of Alkaline Water Electrolysis. *J. Appl. Electrochem.* **2012**, *42* (8), 545–554. https://doi.org/10.1007/s10800-012-0432-2.

(18) Karas, F.; Hnát, J.; Paidar, M.; Schauer, J.; Bouzek, K. Determination of the Ion-Exchange Capacity of Anion-Selective Membranes. *Int. J. Hydrogen Energy* **2014**, *39* (10), 5054–5062. https://doi.org/10.1016/j.ijhydene.2014.01.074.

Chapter 4 – Future work

In summary, we have introduced a new platform for the synthesis of a brush-like liquid crystalline anion exchange membranes with imidazolium functionalized nanopores for energy conversion applications. By this novel polymer architecture, the importance of structure-property relationship to enhance conductivity and mechanical and chemical integrity of an AEM is highlighted. This opens the insight for new research to explore the further modifications and developments that could be done in the field of synthesis of AEMs meeting the demands of the global energy production.

4.1 Modifications of the membranes for Industrial Applications

The synthesized triblock copolymers have to be further characterized using Transmission electron microscopy(TEM), Small-angle X-ray diffraction (SAX) to get a better understanding of the morphology and the distribution of nanopores. [1,2]Compared to SEM, TEM provides more information about the internal morphology and by this further modification that has to be done to obtain interconnected ion channels could be identified.

Also, the etching and crosslinking conditions have to be optimized in order to obtain an even distribution of nanopores and high mechanical integrity respectively. The selective etching of the PLA domains has a high impact on tailoring the properties of the microstructure of the triblock copolymers introduced. Hence by optimizing the etching conditions well defined nanoporous structure with interconnected ion channels could be obtained. [3] Also, it has been found that stiffness-toughness balance of PLA domains play an important role in determining the membrane durability and heat resistance.[4]

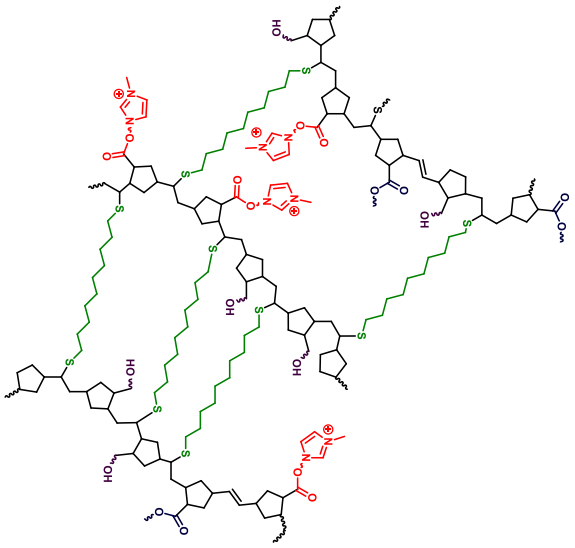

Figure 4. 1: Schematic illustration of the crosslinked structure

The crosslinking percentage basically controls the mechanical properties of the membrane but if increased greatly it could affect the ionic mobility leading to low ion conductivity. Quantification of the mechanical strength has to be done using techniques such as Dynamic-mechanical thermal analysis (DMTA) prior commercialization of the membranes. Moreover, an idea of the amount of membrane swelling could be obtained by water uptake calculation at different humidity conditions and thereby could roughly calculate the needed crosslinking percentage.[5,6] The water uptake of a membrane can be calculated using the following equation where, WU, W_{wet} and W_{dry} means the water uptake, wet mass of the membrane and dry mass of the membrane respectively.

$$WU = \frac{W_{wet} - W_{dry}}{W_{dry}} \times 100\%$$

4.2 Ion conductivity measurements

The IEC gives an insight into the number of ion exchanging site per gram of the dry membrane and it gives an idea of the ion conductivity also. But before using these membranes for industrial applications the ion conductivity should be quantified. This could be done via four-probe cell where the membrane is sandwiched between the two graphite cell blocks to form an air-tight enclosure equipped with an inlet and an outlet for the conditioning gas stream over the membrane sample.[1]

4.3 The effect of the spacer length

Most prior studies conducted on AEMs have highlighted the need of a good microphase separation to enhance ionic conductivity and one approach to induce microphase segregation is to have the ion exchanging head group attached to the polymer backbone via regularly spaced polymer backbones[7,8,9]. Effect of the spacer length has a high impact on microphase separation as well as ionic mobility. We have synthesized the imidazolium functionalized ion-conducting block with a spacer length of 6 CH_2 units in this study and the effect of the length of the spacer group will be studied using 3 spacer and 12 spacer monomers. (Figure 4.2)

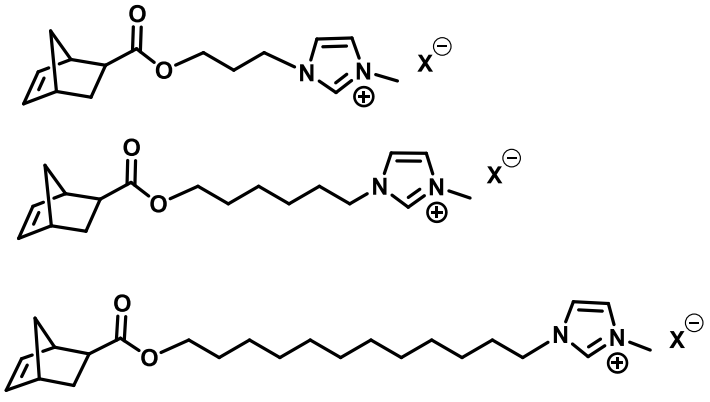

Figure 4. 2: Proposed structures of the monomers with various spacer lengths

4.4 Effect of the counter ion

Synthesis route of the monomer NB IM Br as described in section 3.3.2 D, allows us to change the counter ion of the monomer easily by simple organic reactions. Some counter ions bind to the ion exchanging site strongly while some do not. Hence by changing the counter ion attached, we could determine the effect of counterion on ion conductivity and the membrane degradation.

4.5 Incorporating the AEM in a bipolar membrane synthesis

By definition bipolar membrane is an ion exchange membrane where a cation exchange layer is laminated with an anion exchange layer by an intermediate layer. These have gained immense interest in the recent past due to its high efficiency in fuel cell and electrodialysis applications. [9,10,11]Earlier our group has introduced an amine-functionalized nanoporous cation exchange membrane [12] (Figure 4.2) and once this AEM is characterized and optimized it can be laminated with the aforementioned CEM to produce a bipolar membrane. This opens novel doors to be explored in the field of energy conversion method.

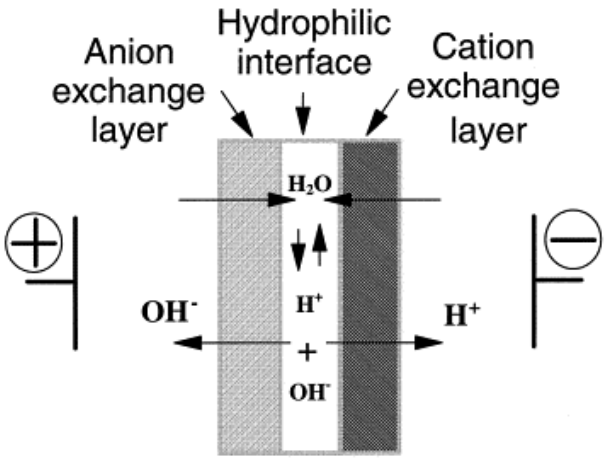

Figure 4. 3: Schematic illustration of a bipolar membrane

Bipolar membranes are widely used in the field of water electrolysis where water is electrically split into hydrogen ions and hydroxide ions without generation of any gases. Also, they are used in low energy chemical manufacturing and separation processes such as acid-base synthesis, purification of acids and bases, separation of mono and divalent ions and desalination.[13,14]

Water splitting by bipolar membranes has gained much attention mainly due to its low energy consumption during the process. The energy consumption for conventional electrolysis is 198.5 kJ/mol, while for water splitting by bipolar membranes it is only 79.9 kJ/ mol. Also, the necessity for cooling reduces as less heat is generated due to low energy consumption. In addition, bipolar membrane water splitting does not produce any gases such as hydrogen, oxygen and chlorine which diminishes the corrosion of the electrodes.[14]

To obtain high-performance bipolar membranes, different methods are used. One common method is the direct adhesion of the cation and anion exchange membranes with an adhesive paste or hot pressure. The other methods include solution casting and electrospinning. Out of these electrospinning has shown the greatest promise due to its ability to control layer thickness. It has been found that by electrospinning the thickness of the bilayer and the interface could be regulated quantitatively.[15,16,17]

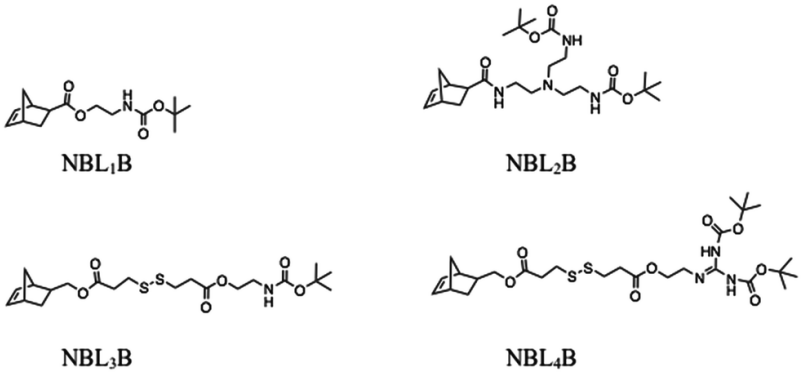

Figure 4. 4: Monomers introduced by our group that can be used as cation exchange membranes (Adapted from reference 12)

Also, these could be prepared by in-situ simultaneous grafting of the same porous material and selectively functionalize the sides later. As a start, we will be preparing the bipolar membranes by the conventional adhesion method because it is a well-studied method for crosslinked polymers. However, there are some technical issues associated with the adhesion method. Basically, one common solvent is used and there is a high chance of both the membranes being soluble in that solvent. Therefore Hence the layers to be cast together should be chosen carefully. Using hot pressure adhesion method could be used as an alternative but it is sometimes hard to alter the thickness of the intermediate layer which adjusts the membrane resistance and water dissociation voltage.[15]

In this case, electrospinning provides a better solution but crosslinked polymers cannot be used due to solubility issues. One possible approach is to use PLA removed cation exchange membrane and anion exchange membranes to make fibers and then crosslink. Usually, post-polymerization reactions are difficult to control and if not carefully done it could cause other problems. The main advantage of the electrospinning method is it gives two hierarchies of pores, (1) due to selective removal of PLA (2) pores from spun fibers. This increase the surface area of the substrate where the electro-oxidation reaction takes place and enhances the ion conductivity. This is a whole new area of research and without doing it experimentally the best preparation method for the suggested CEM and AEM is hard to be postulated.

4.6 References

(1) S. C. Price,a X. Ren,b A. M. Savagea, F. L. B. Synthesis and Characterization of Anion-Exchange Membranes Based on Hydrogenated Poly(Norbornene). *Polym. Chem.* **2017**, *8* (37), 5708–5717. https://doi.org/10.1039/C7PY01084B.

(2) Ayers, K. E.; Anderson, E. B.; Capuano, C. B.; Niedzwiecki, M.; Hickner, M. A.; Wang, C.-Y.; Leng, Y.; Zhao, W. Characterization of Anion Exchange Membrane Technology for Low Cost Electrolysis. *ECS Trans.* **2013**, *45* (23), 121–130. https://doi.org/10.1149/04523.0121ecst.

(3) Deshmukh, P.; Gopinadhan, M.; Choo, Y.; Ahn, S. K.; Majewski, P. W.; Yoon, S. Y.; Bakajin, O.; Elimelech, M.; Osuji, C. O.; Kasi, R. M. Molecular Design of Liquid Crystalline Brush-like Block Copolymers for Magnetic Field Directed Self-Assembly: A Platform for Functional Materials. *ACS Macro Lett.* **2014**. https://doi.org/10.1021/mz500161k.

(4) Nagarajan, V.; Mohanty, A. K.; Misra, M. Perspective on Polylactic Acid (PLA) Based Sustainable Materials for Durable Applications: Focus on Toughness and Heat Resistance. *ACS Sustainable Chemistry and Engineering*. 2016, pp 2899–2916. https://doi.org/10.1021/acssuschemeng.6b00321.

(5) Zheng, Y.; Ash, U.; Pandey, R. P.; Ozioko, A. G.; Ponce-González, J.; Handl, M.; Weissbach, T.; Varcoe, J. R.; Holdcroft, S.; Liberatore, M. W.; et al. Water Uptake Study of Anion Exchange Membranes. *Macromolecules* **2018**, *51* (9), 3264–3278. https://doi.org/10.1021/acs.macromol.8b00034.

(6) Luo, X.; Wright, A.; Weissbach, T.; Holdcroft, S. Water Permeation through Anion Exchange Membranes. *J. Power Sources* **2018**, *375*, 442–451. https://doi.org/10.1016/j.jpowsour.2017.05.030.

(7) Dang, H. S.; Weiber, E. A.; Jannasch, P. Poly(Phenylene Oxide) Functionalized with Quaternary Ammonium Groups via Flexible Alkyl Spacers for High-Performance Anion Exchange Membranes. *J. Mater. Chem. A* **2015**, *3* (10), 5280–5284. https://doi.org/10.1039/c5ta00350d.

(8) Lin, C. X.; Huang, X. L.; Guo, D.; Zhang, Q. G.; Zhu, A. M.; Ye, M. L.; Liu, Q. L. Side-Chain-Type Anion Exchange Membranes Bearing Pendant Quaternary Ammonium Groups: Via Flexible Spacers for Fuel Cells. *J. Mater. Chem. A* **2016**, *4* (36), 13938–13948. https://doi.org/10.1039/c6ta05090e.

(9) Lee, W. H.; Kim, Y. S.; Bae, C. Robust Hydroxide Ion Conducting Poly(Biphenyl Alkylene)s for Alkaline Fuel Cell Membranes. *ACS Macro Lett.* **2015**, *4* (8), 814–818. https://doi.org/10.1021/acsmacrolett.5b00375.

(10) Tanaka, Y. Chapter 3 Bipolar Membrane Electrodialysis. *Membrane Science and Technology*. 2007, pp 405–436. https://doi.org/10.1016/S0927-5193(07)12017-9.

(11) Trivedi, G. S.; Shah, B. G.; Adhikary, S. K.; Indusekhar, V. K.; Rangarajan, R. Studies on Bipolar Membranes. *React. Funct. Polym.* **1996**, *28* (3), 243–251. https://doi.org/10.1016/1381-5148(95)00088-7.

(12) Ndaya, D.; Bosire, R.; Mahajan, L.; Huh, S.; Kasi, R. Synthesis of Ordered, Functional, Robust Nanoporous Membranes from Liquid Crystalline Brush-like Triblock Copolymers. *Polym. Chem.* **2018**, *9* (12), 1404–1411. https://doi.org/10.1039/c7py02127e.

(13) Xu, T. Development of Bipolar Membrane-Based Processes. *Desalination* **2001**, *140* (3), 247–258. https://doi.org/10.1016/S0011-9164(01)00374-5.

(14) Huang, C.; Xu, T. Electrodialysis with Bipolar Membranes for Sustainable Development. *Environmental Science and Technology*. 2006, pp 5233–5243. https://doi.org/10.1021/es060039p.

(15) Pan, J.; Hou, L.; Wang, Q.; He, Y.; Wu, L.; Mondal, A. N.; Xu, T. Preparation of Bipolar Membranes by Electrospinning. *Mater. Chem. Phys.* **2017**, *186*, 484–491. https://doi.org/10.1016/j.matchemphys.2016.11.023.

(16) Lobyntseva, E.; Kallio, T.; Kontturi, K. Bipolar Membranes in Forward Bias Region for Fuel Cell Reactors. *Electrochim. Acta* **2006**, *51* (7), 1165–1171. https://doi.org/10.1016/j.electacta.2005.06.004.

(17) Jeevananda, T.; Yeon, K. H.; Moon, S. H. Synthesis and Characterization of Bipolar Membrane Using Pyridine Functionalized Anion Exchange Layer. *J. Memb. Sci.* **2006**, *283* (1–2), 201–208. https://doi.org/10.1016/j.memsci.2006.06.029.